JOURNAL OF GEOPHYSICAL RESEARCH, VOL. 95, NO. B13, PAGES 21,931–21,948, DECEMBER 10, 1990

Present-day Kinematics of the Rivera Plate and Implications for Tectonics in Southwestern Mexico

CHARLES DEMETS

Jet Propulsion Laboratory, California Institute of Technology, Pasadena

SETH STEIN

Department of Geological Sciences, Northwestern University, Evanston, Illinois

We model the present-day motion of the Rivera plate relative to the Pacific, North America, and Cocos plates, and combine the results with the NUVEL-1 model for Cocos–North America motion to examine present-day deformation in southwestern Mexico. The Pacific–Rivera data, which include 25 three m.y.-average spreading rates determined from original surface-ship magnetic data and 22 azimuthal data along the Rivera transform, are systematically misfit by the NUVEL-1 Pacific–North America and Pacific–Cocos Euler vectors, indicating that the Rivera plate is kinematically distinct from North America and Cocos. An F test shows that the improvement in fit to the Pacific–Rivera data from a model with a distinct Rivera plate exceeds that expected solely from adding three model parameters. The Rivera–North America Euler vector derived from closure of the Rivera–Pacific–North America plate circuit predicts slower and more trench-normal convergence along the Acapulco trench than prior models. In addition, the model predicts convergence normal to the eastern Tamayo fracture zone at a rate 60% slower than the right-lateral strike-slip predicted by prior models. An observed systematic misfit of the Pacific–Rivera Euler vector to azimuths from the western Rivera transform fault may have several causes. There may be a time-averaging problem between the 3.0-m.y.-average rates and the shorter time-average transform fault azimuths and earthquake slip vectors. Alternatively, Rivera transform trends may be biased by deformation within lithosphere adjacent to the transform valley, or future detailed mapping of the transform may reveal the misfit to be an artifact of the presently available bathymetry. Along the entire Pacific–Rivera rise, spreading rates averaged over the past 0.7 m.y. are systematically faster than 3.0-m.y.-average rates, with the difference increasing southward along the rise. The post-3 Ma change in the rate gradient has caused a southward migration of the Pacific–Rivera Euler pole since 3 Ma, possibly in response to the ~3 Ma completion of a spreading reorganization that doubled the length of the Rivera transform fault and halved the area of the Rivera plate. We hypothesize that deformation in southwestern Mexico, including opening along the Colima rift, is related to oblique subduction of the Cocos plate along the northern Middle America trench. Three lines of evidence support this hypothesis. First, the sense of oblique subduction predicted by NUVEL-1 along the Middle America trench is consistent with a model in which part of western Mexico located southeast of the Colima rift moves to the southeast relative to North America. Second, field geologic data and Landsat imagery suggest that in the past few million years, the Chapala-Oaxaco fault zone has accommodated several kilometers of sinistral motion and sinistral transtension has occurred along the Trans-Mexican Volcanic Belt. Either or both of these fault zones could accommodate any southeastward coastal block motion that might result from oblique subduction. Third, the observation that earthquake slip vectors from the northern Middle America trench trend systematically counterclockwise from the predicted Cocos–North America convergence direction is also consistent with southeastward motion. The discrepancy between the observed and predicted slip directions along the Middle America trench suggests sinistral slip is 0–10 mm yr^{-1}. If oblique subduction is driving southeastward transport of a coastal sliver, the Colima rift is a passive, pull-apart zone at the northwestern end of this sliver, rather than an incipient spreading ridge that will replace the Pacific–Rivera rise.

INTRODUCTION

An understanding of the cause, distribution, and timing of Cenozoic and late Mesozoic volcanism and deformation along the western margin of the Americas requires accurate models of the present-day and past motions of the Farallon plate and the remnants of its post-56 Ma breakup, the Rivera, Cocos, Nazca, Juan de Fuca, and Explorer plates, which have been subducting beneath the western Americas for more than 100 m.y. *Menard* [1978] speculated that pivoting subduction of fragments of the Farallon plate may influence volcanism and crustal deformation in Mexico, and kinematic models for the Farallon plate have been used to explain Laramide deformation and volcanism in western North America [*Coney and Reynolds*, 1977; *Cross and Pilger*, 1978; *Henderson and Gordon*, 1984]. Models for present-day plate motions are also proving useful for studying continental tectonics. For instance, kinematic models of present-day Pacific–North America motion place important constraints on deformation integrated across the Basin and Range province and California [*Minster and Jordan*, 1984; *DeMets et al.*, 1987, 1990].

Here we derive a model for the present-day motion of the Rivera plate relative to the neighboring plates, North America, Cocos, and Pacific, and examine the implications of a model for Rivera and Cocos plate subduction along the Middle America trench for present-day deformation in southwestern Mexico. Studies of seismicity in Mexico and along the Middle America trench [*Eissler and McNally*, 1984; *Singh et al.*, 1985; *Anderson et al.*, 1989] and studies of Plio-Pleistocene

Paper number 90JB01836.
0148-0227/90/90JB-01836$05.00

volcanism and deformation in southwestern Mexico suggest that slow subduction of the Rivera plate and somewhat faster subduction of the adjacent Cocos plate influence volcanism and deformation in southwestern Mexico [*Luhr et al.*, 1985; *Allan*, 1986; *Johnson and Harrison*, 1989; *Allan et al.*, 1990]. Accurate models for present-day Rivera plate motion and Cocos–North America motion [*DeMets et al.*, 1990] thus provide an indirect way to investigate deformation in Mexico.

To study the recent evolution of Rivera plate motions, we determine Pacific–Rivera plate velocities over three averaging intervals, 0.7, 1.7, and 3.0 m.y., which is the averaging interval used to derive the closure-consistent NUVEL-1 global plate motion model [*DeMets et al.*, 1990]. Although two models of present-day (e.g., 3.0 m.y.-average) Pacific–Rivera plate motion are available [*Minster and Jordan*, 1979; *Klitgord and Mammerickx*, 1982], we construct a new model for two reasons. First, new data from the Pacific–Rivera rise and Rivera transform fault permit a more accurate estimate of Pacific–Rivera motion and its uncertainties. Second, recent estimates of present-day Pacific–North America and Pacific–Cocos motions [*DeMets et al.*, 1987, 1990] differ significantly from those previously used [*Minster and Jordan*, 1978] to estimate motion of the Rivera plate relative to the North America and Cocos plates.

As part of this analysis, we reconsider several questions raised in previous studies of the Rivera plate [*Atwater*, 1970; *Larson*, 1972; *Sharman et al.*, 1976; *Minster and Jordan*, 1979; *Klitgord and Mammerickx*, 1982; *Eissler and McNally*, 1984]. Do plate motion data from the northern East Pacific rise require a distinct Rivera plate? Is subduction of the Rivera plate along the seismically quiescent Acapulco trench (the Middle America trench north of 18.5°N) required by plate kinematic data, and if so, what does the predicted subduction rate imply about the earthquake recurrence interval in the Jalisco region of southwestern Mexico? We also consider several questions not treated in prior studies. Has Pacific–Rivera motion changed in the past 3 m.y.? Could oblique subduction along the Middle America trench be related to geologically observed sinistral slip along faults in southwestern Mexico and extension across the Colima, Tepic-Chapala (also known as the Tepic-Zacoalco), and Chapala rifts in the Jalisco province of southwestern Mexico?

Tectonic Setting of the Rivera Plate

The tectonic setting of the tiny Rivera plate (~100,000 km^2) is complex (Figure 1). Only the Pacific–Rivera rise and Rivera transform fault (Figure 1), which record Rivera–Pacific motion, are well understood and yield data suitable for constructing a kinematic model. The Pacific–Rivera rise is accurately located from marine magnetic and bathymetric data (Figure 2). The average profile spacing along the 360-km-long rise is 10 km, 5–10 times more closely spaced than magnetic profiles across most mid-ocean ridges.

The Rivera Transform Fault

The Rivera transform fault, which offsets the southern Pacific–Rivera rise and northern Pacific–Cocos rise, took its present arcuate shape at about anomaly 3 time, when spreading along the Mathematician rise transferred to the northern Pacific–Cocos rise [*Klitgord and Mammerickx*, 1982; *Mammerickx*, 1984; *Mammerickx et al.*, 1988]. East of 107.5°W, a Seabeam survey shows two parallel transform valleys trending ~N70°W [*Bourgois et al.*, 1988*a*]. The northern valley is sedimented and is thus interpreted by Bourgois et al. to be inactive. Several magnitude 5.0 and larger earthquakes (Figure 1) appear to be located in the northern transform valley [*Eissler and McNally*, 1984], so some slip may still occur along these faults. In the southern valley, which contains little sediment, multiple fault traces connected by 1–2 km wide relay zones (bold line in Figure 1) probably accommodate present-day strike-slip motion [*Bourgois et al.*, 1988*a*]. Pacific–Rivera strike-slip motion may cease east of 18.50°N, 106.25°W, where an isolated north trending rise segment identified from Seabeam data [*Bourgois et al.*, 1988a] intersects the southern transform valley. This rise segment is separated from the northern Pacific–Cocos rise by a region of diffuse seismicity south of the eastern Rivera fracture zone (Figure 1). Along the Rivera transform west of 107.5°W, seismicity is more diffuse and conventional bathymetry reveals several subparallel valleys [*Dauphin and Ness*, 1990]. The fault or faults that accommodate present-day slip cannot be determined from the available seismicity or bathymetry; however, the trends of the transform valleys and the slip directions of strike-slip earthquakes west of 107.5°W are predominantly N50°W-N60°W.

The Rivera–North America Boundary

The Rivera–North America boundary can be divided into two distinct regions. The Acapulco trench, which is located west of the Colima rift and north of the Rivera fracture zone (Figure 1), extends to 21°N [*Fisher*, 1961]. Although *Larson* [1972] interprets the low present level of seismicity along the Acapulco trench and small sediment fill shown by seismic reflection profiles across the Tres Marias escarpment and Acapulco trench [*Ross and Shor*, 1965; *Moore and Buffington*, 1968] as evidence that subduction has ceased in the past few million years, the Acapulco subduction zone is still active and constitutes a seismic hazard [*Kanamori*, 1987]. A 300 km segment of the Acapulco trench ruptured during the M_s=8.2 June 3, 1932 and M_s=7.8 June 18, 1932 earthquakes [*Singh et al.*, 1985]. These two earthquakes and their aftershocks occurred along the continental margin west of the Colima rift, coincident with the Acapulco trench [*Eissler and McNally*, 1984; *Singh et al.*, 1985]. Earthquake mechanism 32 (Figure 1; Table 1) is further evidence that subduction along the Acapulco trench is active. North of 21°N, few observations constrain the location or sense of deformation associated with Rivera–North America motion. Some seismicity along the Tres Marias escarpment and near the eastern Tamayo fracture zone may indicate that these two features accommodate Rivera–North America motion. Because no focal mechanisms for large earthquakes along the Rivera–North America boundary are available, no data from this boundary are used to derive the kinematic model.

The Cocos–Rivera Boundary

Little is known about the Rivera–Cocos and Pacific–Cocos boundaries near 18.5°N, 105.7°W, where the three plates should meet. Diffuse seismicity in the region suggests that a simple three plate model does not fully describe the local relative motions, and a Seabeam survey of the northern Middle America trench and Acapulco trench indicates that neither the Pacific–Cocos nor Cocos–Rivera plate boundaries near the tri-

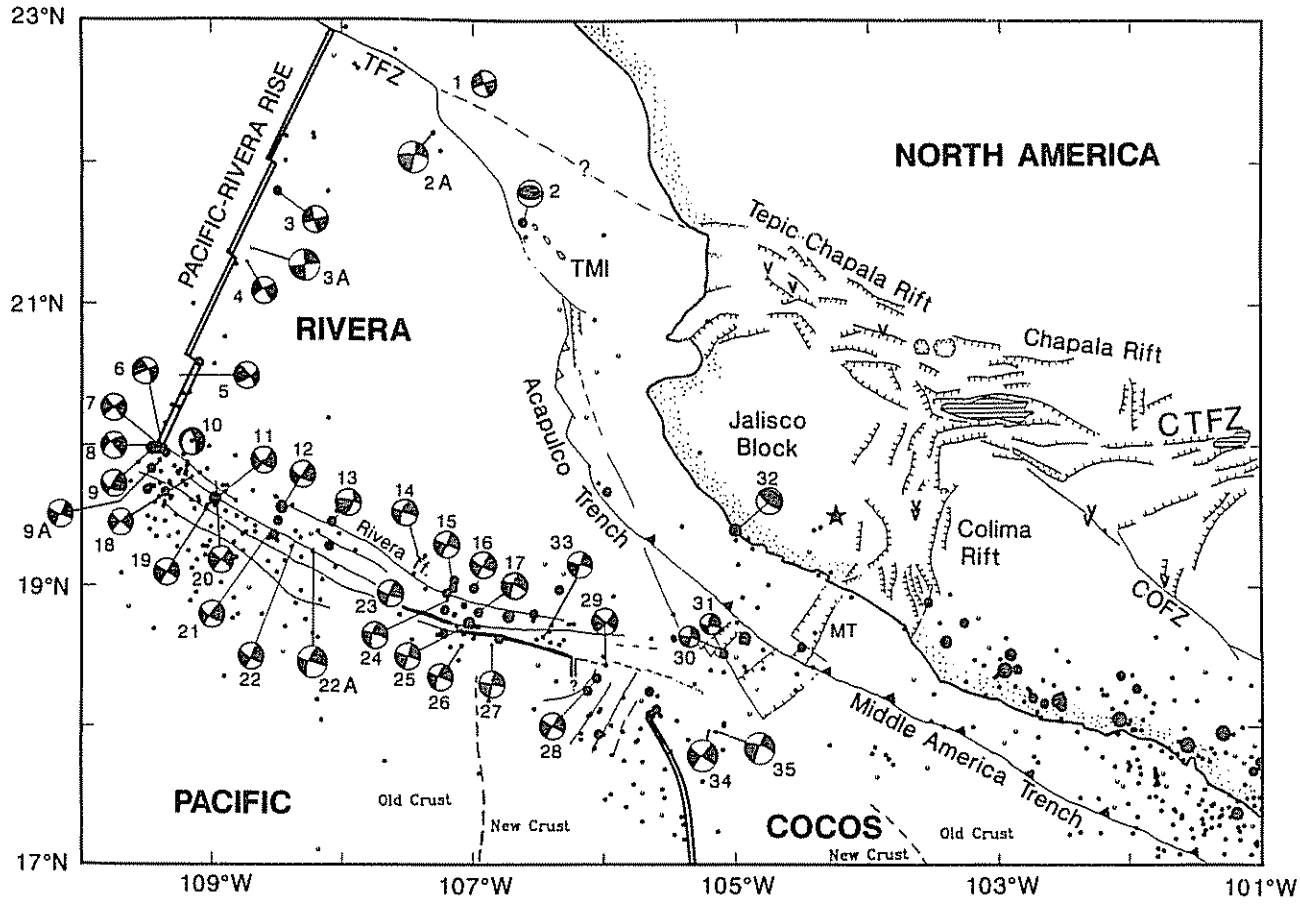

Fig. 1. Neotectonics of the Rivera plate region. Onshore normal faults (hachured lines) are from *Allan et al.* [1990] and *Harrison and Johnson* [1988]. Seafloor bathymetric and tectonic features are compiled from *Klitgord and Mammerickx* [1982], *Dauphin and Ness* [1990], and *Bourgois et al.* [1988*a*,*b*]. East of 107.4°W, the active Rivera transform fault strand identified from Seabeam data is shown with a bold line; inactive faults are dashed. The star shows the preferred location for the 1932 Jalisco earthquake [*Eissler and McNally*, 1984] and Vs show locations of active volcanoes [*Harrison and Johnson*, 1988]. Small solid circles show all shallow (<50 km) earthquakes recorded between January, 1967 and December, 1986 from the National Geophysical Data Center Earthquake data file. Medium and large solid circles show all 1964–1976 earthquakes with magnitudes larger than 4.8 that have been relocated by *Eissler and McNally* [1984]. Earthquake focal mechanisms are listed in Table 1. Abbreviations are MT, Manzanillo trough; COFZ, Chapala-Oaxaca fault zone; CTFZ, Chapala-Tula fault zone; TMI, Tres Marias Islands; TFZ, Tamayo fracture zone.

ple junction are discrete [*Mammerickx*, 1984; *Bourgois et al.*, 1988*b*]. *Eissler and McNally* [1984] suggest that the Rivera–Cocos boundary may be a NE trending, left-lateral strike-slip boundary connecting the Rivera transform to the Middle America trench. Alternatively, one or more E-W dextral strike-slip faults may connect the northern end of the Pacific–Cocos rise to the Middle America trench [*Bandy et al.*, 1988]. Four earthquake focal mechanisms (30, 31, 34, 35 in Table 1 and Figure 1) do not rule out either of the proposed geometries.

Although no discrete Cocos–Rivera boundary has been found, two grabens within soon-to-be subducted lithosphere near the Pacific–Rivera–Cocos triple junction (Figure 1) were located during a Seabeam, gravity, magnetic, and seismic survey [*Bourgois et al.*, 1988*b*] (Figure 1). Bourgois et al. postulate that rifting along these two grabens is related to extension along the Colima rift and Manzanillo trough east of the trench. However, if subduction along the Acapulco trench is still active, then deformation within oceanic lithosphere west of the trench is probably unrelated to rifting within continental North American lithosphere east of the trench. Deformation immediately west of the trench may instead be related to interaction between the Rivera and Cocos plates before subducting beneath western Mexico.

Because no data unambiguously define the plate geometry near the triple junction, no data from this region are used to derive Rivera plate motions.

Southern Mexico

Given that the Rivera–North America boundary is so poorly defined, consideration of landward deformation is relevant. Field work, mapping from air photos, and Landsat Thematic Mapper images have defined active faults along the Tepic-Chapala, Colima, and Chapala rifts in southwestern Mexico that may be related to Rivera–North America tectonics [*Allan*, 1986; *Johnson and Harrison*, 1989; *Allan et al.*, 1990].

Radiometric ages for volcanics along the Colima and Tepic-Chapala rifts indicate that the most recent pulse of volcanism began about 5 Ma [*Allan*, 1986], with some dates sug-

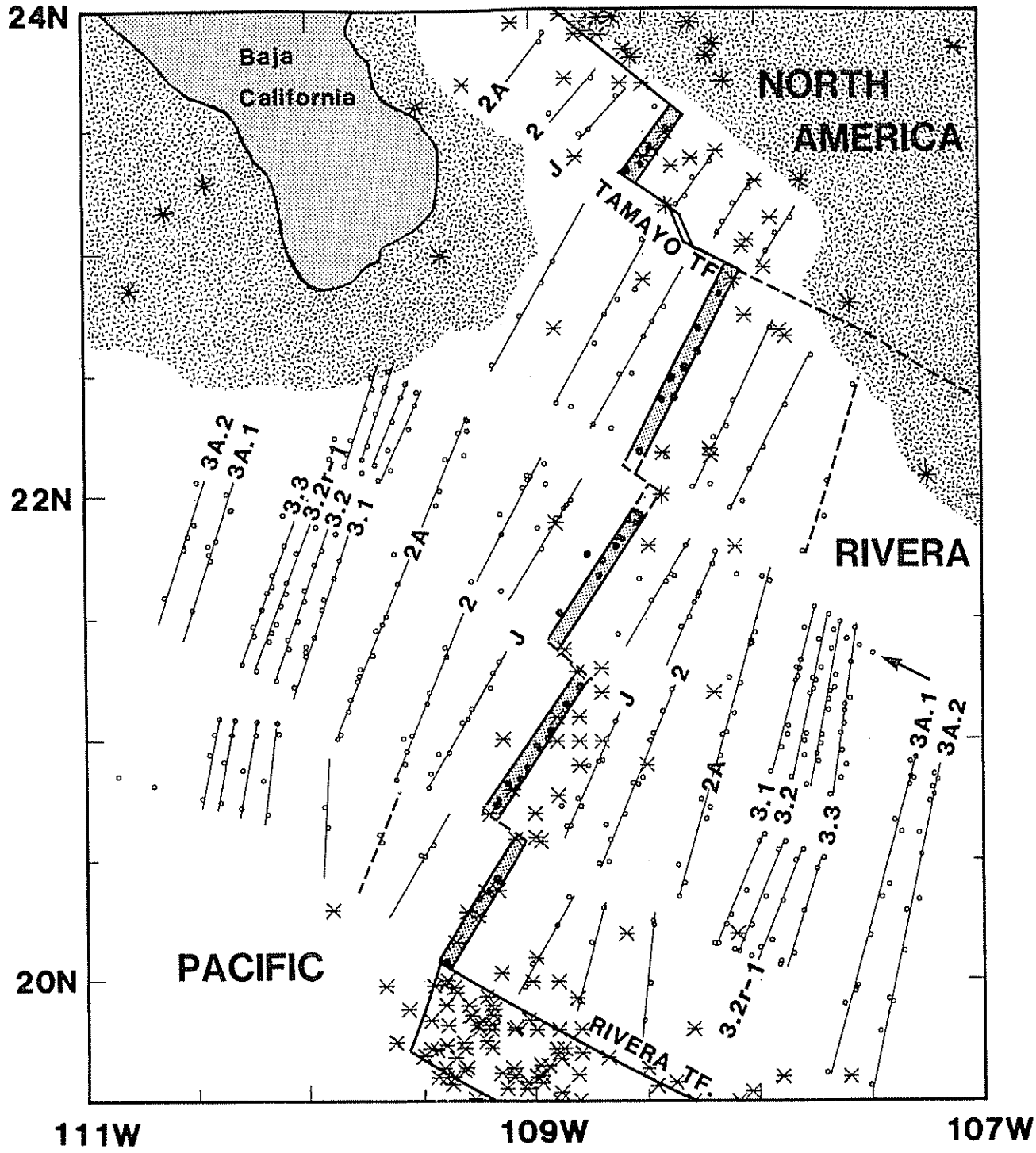

Fig. 2. Magnetic anomaly correlations along the Pacific–Rivera rise. Small circles show age correlations; lineation trends are interpreted from the age picks. Correlations are shown for the following reversals: The axial magnetic high (0.0 Ma), Jaramillo (0.95 Ma), anomaly 2 (1.76 Ma), the center of anomaly 2A (3.00 Ma), and anomalies 3.1, 3.2, 3.2r-1, 3.3, 3A.1, and 3A.2 (3.89, 4.17, 4.46, 4.69, 5.54, and 5.95 Ma, respectively). Stippled areas delineate the limits of the continental slope. Asterisks show all shallow (< 50 km) earthquakes recorded between January, 1963 and December, 1986. The arrow points to one track with anomalies that are systematically mislocated relative to nearby satellite-positioned data.

gesting volcanism as early as 11 Ma. The total extensions across the northern Colima rift and eastern Tepic-Chapala rifts, 1.5–3 km and 2–4 km respectively [*Allan*, 1986], imply extension rates slower than 1 mm yr^{-1}, although *Allan et al.* [1990] suggest that the total extension across the southern Colima rift is greater than across the northern Colima rift. The slow extension rates are consistent with the near absence of seismicity along any of the rifts, although some aseismic deformation could occur. Any strike-slip motion along these rifts will also contribute to the total deformation. Because extension

TABLE 1. Epicentral Data and Source Parameters

No.	Date	Latitude, °N	Longitude, °W	M_o 10^{24} dyn cm	Mechanism†	Source
01	Dec. 8, 1982	22.58	106.91	0.2	160/90/180	*Dziewonski et al.* [1988*a*]
02	Feb. 9, 1976	21.63	106.59	7.1	92/52/086	*Goff et al.* [1987]
02A	Jan. 31, 1989	22.18	107.29	1.7	276/74/173	*Dziewonski et al.* [1990*a*]
03	Aug. 24, 1985	21.75	108.42	2.5	165/81/-177	*Dziewonski et al.* [1986]
03A	Feb. 10, 1989	21.40	108.70	2.0	265/90/180	*Dziewonski et al.* [1990*a*]
04	May 22, 1966	21.30	108.70	5.4 m_b	148/90/180	*Sykes* [1970]
05	Feb. 17, 1984	20.50	109.23	14	57/72/16	*Dziewonski et al.* [1984]
06	May 8, 1983	19.99	109.41	1.8	336/69/-17	*Dziewonski et al.* [1988*a*]
07	May 8, 1983	19.95	109.35	2.9	141/90/180	*Dziewonski et al.* [1988*a*]
08	May 8, 1983	20.00	109.34	7.2	141/87/150	*Dziewonski et al.* [1983]
09	May 9, 1983	19.98	109.45	42	210/82/041	*Dziewonski et al.* [1983]
09A	Jan. 23, 1967	19.88‡	109.45‡	5.3 m_b	117/85/180	*Molnar* [1973]
10	Sept. 21, 1977	20.03	109.15	6.6	346/72/-106	*Dziewonski et al.* [1987*a*]
11	Jan. 25, 1985*	19.62	108.97	1.5	38/83/-20	*Dziewonski et al.* [1985]
12	July 8, 1985*	19.56	108.46	8.1	213/88/24	*Dziewonski et al.* [1986]
13	Aug. 8, 1966*	19.46‡	108.07‡	5.3 m_b	20/63/17	*Molnar* [1973]
14	June 3, 1969*	19.18‡	107.41‡	5.1 m_b	195/70/000	*Molnar* [1973]
15	Dec. 6, 1965*	18.99‡	107.15‡	5.9 m_b	202/86/000	*Sykes* [1967]
16	Sept. 23, 1969	18.99‡	106.99‡	5.0 m_b	116/80/180	*Molnar* [1973]
17	July 23, 1968*	18.82‡	106.96‡	5.4 m_b	296/80/180	*Molnar* [1973]
18	Jan. 10, 1988*	19.77	109.17	3.2	220/87/000	*Dziewonski et al.* [1989*b*]
19	Nov. 14, 1987*	19.68	108.99	51	301/90/180	*Dziewonski et al.* [1989*a*]
20	Nov. 14, 1987*	19.76	108.96	3.4	309/90/180	*Dziewonski et al.* [1989*a*]
21	Jan. 4, 1986*	19.39	108.55	2.7	216/82/22	*Dziewonski et al.* [1987*b*]
22	Jan. 1, 1986*	19.32	108.36	2.6	30/85/-13	*Dziewonski et al.* [1987*b*]
22A	May 13, 1989*	19.25	108.70	0.2	199/69/002	*Dziewonski et al.* [1990*b*]
23	Nov. 1, 1980*	18.95	107.63	40	108/78/174	*Dziewonski et al.* [1988*b*]
24	Dec. 7, 1986*	18.90	107.20	18	288/83/-161	*Dziewonski et al.* [1987*c*]
25	June 1, 1981*	18.73	107.03	25	18/90/000	*Dziewonski and Woodhouse* [1983]
26	Nov. 27, 1987*	18.55	107.13	2.4	201/74/000	*Dziewonski et al.* [1989*a*]
27	Nov. 9, 1986*	18.57	106.86	1.4	280/90/180	*Dziewonski et al.* [1987*c*]
28	July 24, 1968	18.34‡	106.06‡	5.0 m_b	120/90/180	*Molnar* [1973]
29	Oct. 25, 1982	18.43	105.99	1.7	41/79/001	*Dziewonski et al.* [1988*a*]
30	Jan. 22, 1973	18.54	105.11	6.1 M_s	99/86/190	*Eissler and McNally* [1984]
31	June 26, 1967	18.47‡	105.12‡	5.2 m_b	95/75/161	*Molnar* [1973]
32	Oct. 18, 1973	19.46	104.93	6.0 m_b	305/18/89	*Eissler and McNally* [1984]
33	Aug. 3, 1988*	18.63	106.48	1.8	16/90/000	*Dziewonski et al* [1989*c*]
34	Apr. 19, 1989	17.86	105.23	2.9	127/85/176	*Dziewonski et al* [1990*b*]
35	Apr. 28, 1989	17.83	105.17	2.5	291/73/-173	*Dziewonski et al.* [1990*b*]

USGS epicenters are used for all Dziewonski et al. centroid-moment tensor solutions except February 10, 1989, whose centroid-moment tensor epicenter is adopted for its proximity to the ridge. The USGS location for this epicenter is 21.56°N, 108.25°W.

* Earthquakes used to determine Pacific–Rivera direction (Table 2).

† Strike (degrees clockwise from N)/Dip (degrees clockwise rotation about strike)/Slip (degrees counterclockwise from strike, in nodal plane)

‡ Epicentral location taken from *Eissler and McNally* [1984].

along the Tepic-Chapala and Colima rifts bounding the Jalisco block is so slow, we treat the Jalisco block as part of North America for a determination of the first-order kinematics. Deformation in southwestern Mexico is discussed in more detail later in the paper.

Pacific-Rivera Rates and Directions

We determined Pacific–Rivera motion from three types of data: 3.0-m.y.-average rates determined from surface ship magnetic data across the Pacific–Rivera rise, fault trends determined from bathymetric data from the Rivera transform valley, and the horizontal projections of slip vectors derived from strike-slip earthquake focal mechanisms along the Rivera transform.

All available surface ship magnetic and bathymetric profiles crossing the Pacific–Rivera rise were obtained from the National Geophysical Data Center (NGDC) and reduced to 34 profiles. The magnetic anomalies were correlated with the reversal time scale of *Harland et al.* [1982]. Only anomalies younger than about 6 Ma (anomaly 4) were correlated because only the recent evolution of the Rivera plate is of interest here. Our correlations (Figure 2) agree with previous analyses of subsets of these data [*Larson*, 1972; *Klitgord and Mammerickx*, 1982; *Ness et al.*, 1990]. Correlations from adjacent satellite-navigated and celestially navigated profiles show occasional 2–10 km systematic offsets, comparable to the 2–5 km errors estimated by *Larson* [1972] for celestially navigated data. Anomaly correlations and spreading rates determined from celestially navigated profiles were thus assigned larger errors than those obtained from cruises navigated with satellite fixes. An independent set of satellite-navigated magnetic profiles give a nearly identical anomaly pattern [*Lonsdale*, 1990], but with less along-lineation scatter than derived from pre-satellite navigated profiles.

The Pacific–Rivera magnetic lineations show a progressive 5°–15° clockwise rotation of the rise crest since about 5 Ma. The present-day rise crest, which is well defined by the axial magnetic high [*Klitgord*, 1976], trends N28°-N33°E, perpendicular to the western Rivera transform. Magnetic lineations

and Seabeam bathymetric swaths show at least three short ridge offsets, each of which may accommodate oblique extension rather than strike-slip motion [*Macdonald et al*, 1980; *Lonsdale*, 1989].

To determine spreading rates averaged over the center of anomaly 2A (3.0 Ma), profiles were projected onto the direction orthogonal to anomaly 2A (Table 2), and were compared to synthetic magnetic profiles at 1 mm yr^{-1} increments. Twenty-four of the profiles appear to cross anomaly 2A on both sides of the rise without crossing fracture zones. These profiles give rates ranging from 50 mm yr^{-1} near the northern end of the Pacific–Rivera rise to 57 mm yr^{-1} near its southern end (Table 2, Figures 3 and 4). One additional rate was determined from several partial profiles across the southern 50 km of the rise (Figure 2). The theoretical anomaly skewness [*Blakely and Cox*, 1972], which was computed using the 1978 International Geomagnetic Reference Field for the ambient field, an axial geocentric dipole model for the remanent field,

TABLE 2. Pacific–Rivera Data

Latitude, °N	Longitude, °W	Datum	σ	Model	ι	Ridge Strike	Source
			Pacific–Rivera 3.0-m.y.-Average Spreading Rates				
22.60	108.28	50	5	48.7	0.066	N25°E	NGDC Marsur 78
22.45	108.26	51	5	49.3	0.053	N25°E	NGDC Marsur 77
22.39	108.42	50	3	49.9	0.119	N25°E	NGDC Golfo 81
22.18	108.53	53	5	51.0	0.027	N25°E	NGDC Marsur 78
21.98	108.50	52	5	51.3	0.027	N20°E	NGDC DSDP 63
21.95	108.50	51	4	51.4	0.040	N20°E	NGDC Gam 2
21.92	108.56	52	4	51.6	0.037	N20°E	NGDC Golfo 81
21.86	108.50	54	4	51.8	0.034	N20°E	NGDC Baja 76
21.82	108.59	52	2	52.1	0.119	N20°E	NGDC Iguana 1
21.82	108.59	52	2	52.1	0.119	N20°E	NGDC *Kana Keoki* 7401
21.80	108.64	52	2	52.3	0.112	N20°E	NGDC Coco Tow 4
21.73	108.68	53	2	52.7	0.099	N20°E	NGDC Iguana 5
21.67	108.71	53	2	53.0	0.091	N20°E	NGDC Marsur 78
21.52	108.88	54	4	54.0	0.021	N20°E	NGDC Gam 2
21.43	109.00	55	2	54.6	0.095	N20°E	NGDC Wel 75
21.27	108.93	55	4	55.2	0.029	N20°E	NGDC Gam 2
21.15	108.85	55	2	55.6	0.138	N20°E	NGDC Marsur 78
21.04	108.93	57	2	56.3	0.179	N20°E	NGDC FD 7707
21.00	108.94	58	3	56.5	0.086	N20°E	NGDC Marsur 78
20.97	108.98	55	4	56.7	0.053	N20°E	NGDC Gam 1
20.89	109.03	57	4	57.1	0.063	N20°E	NGDC Cento 1
20.82	109.11	54	5	57.6	0.048	N20°E	NGDC Gam 1
20.81	109.21	57	5	57.8	0.052	N20°E	NGDC Aria 3
20.75	109.15	55	4	57.9	0.086	N20°E	NGDC Marsur 78
20.30	109.30	57	6	60.2	0.079	N20°E	NGDC Marsur 77, Dolpho 2 Tortuga 3
			Rivera Transform Fault Trends				
19.40	108.50	N61°W	5°	N65.8°W	0.193		*Dauphin and Ness* [1990]
18.75	107.25	N72°W	5°	N71.3°W	0.136		*Bourgois et al.* [1988*a*]
18.67	107.00	N74°W	3°	N72.3°W	0.384		*Bourgois et al.* [1988*a*]
18.60	106.45	N78°W	5°	N74.4°W	0.157		*Bourgois et al.* [1988*a*]
			Rivera Transform Fault Slip Vectors				
19.77	109.17	N50°W	20°	N62.8°W	0.019		CMT Jan. 10, 1988
19.68	108.99	N59°W	15°	N63.6°W	0.028		CMT Nov. 14, 1987
19.62	108.97	N52°W	20°	N63.8°W	0.015		CMT Jan. 25, 1985
19.76	108.96	N51°W	20°	N63.6°W	0.016		CMT Nov. 14, 1987
19.34	108.72	N54°W	20°	N65.2°W	0.013		CMT Jan. 4, 1986
19.56	108.46	N56°W	20°	N65.7°W	0.012		CMT July 8, 1985
19.06	108.32	N60°W	20°	N67.0°W	0.010		CMT Jan. 1, 1986
19.25	108.24	N70°W	25°	N67.0°W	0.007		CMT May 13, 1989
19.46	108.07	N70°W	15°	N67.2°W	0.019		*Molnar* [1973] Aug. 8, 1966
18.95	107.63	N71°W	15°	N69.6°W	0.016		CMT Nov. 1, 1980
19.18	107.41	N75°W	15°	N71.1°W	0.016		*Molnar* [1973] June 3, 1969
18.90	107.20	N74°W	15°	N71.2°W	0.015		CMT Dec. 7, 1986
18.99	107.15	N68°W	15°	N71.3°W	0.016		*Sykes* [1967] Dec. 6, 1965
18.55	107.13	N70°W	20°	N72.0°W	0.008		CMT Nov. 27, 1987
18.73	107.03	N72°W	15°	N72.1°W	0.015		CMT June 1, 1981
18.82	106.96	N67°W	15°	N72.2°W	0.016		*Molnar* [1973] July 23, 1968
18.57	106.86	N80°W	20°	N72.9°W	0.009		CMT Nov. 9, 1986
18.63	106.48	N74°W	20°	N74.2°W	0.010		CMT Aug. 3, 1988

Rates and rate uncertainties are in units of millimeters per year. Rates determined from National Geophysical Data Center data are referenced NGDC. Azimuths are measured in degrees clockwise from north. Slip vectors referenced as CMT are determined from centroid-moment tensor solutions. Data importances (ι) measure the relative contributions of data to the model.

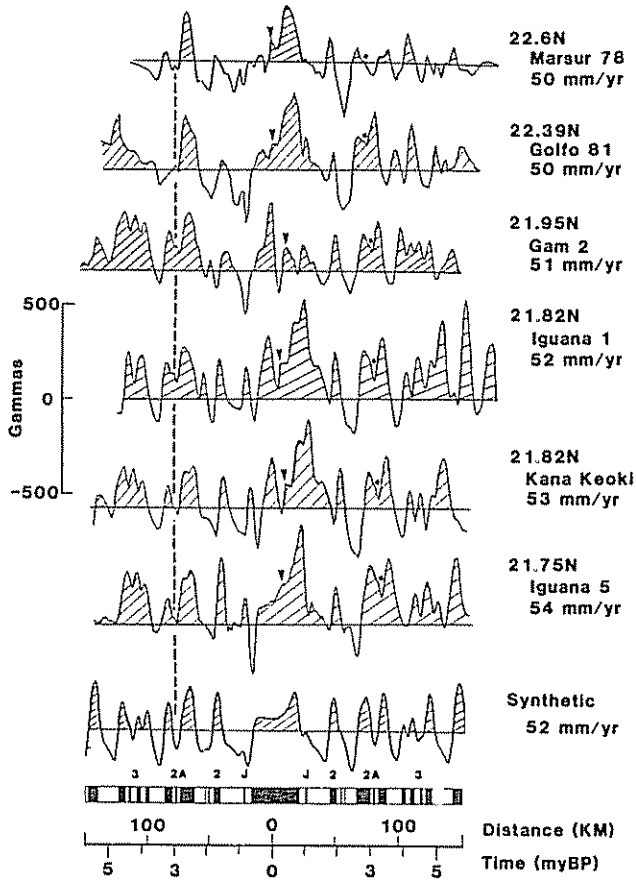

Fig. 3. Magnetic profiles along the northern Pacific–Rivera rise. The profiles, which are projected onto N70°W, are typical of the best profiles along the rise. Comparison with the 52 mm yr^{-1} synthetic profile (bottom) suggests a southward increasing rate. The center of anomaly 2A northwest of the rise is aligned; the center of anomaly 2A southeast of the rise is marked by a small dot. The rise crest, as identified from the axial magnetic high and bathymetry, is marked by an arrow. Left to right represents northwest to southeast.

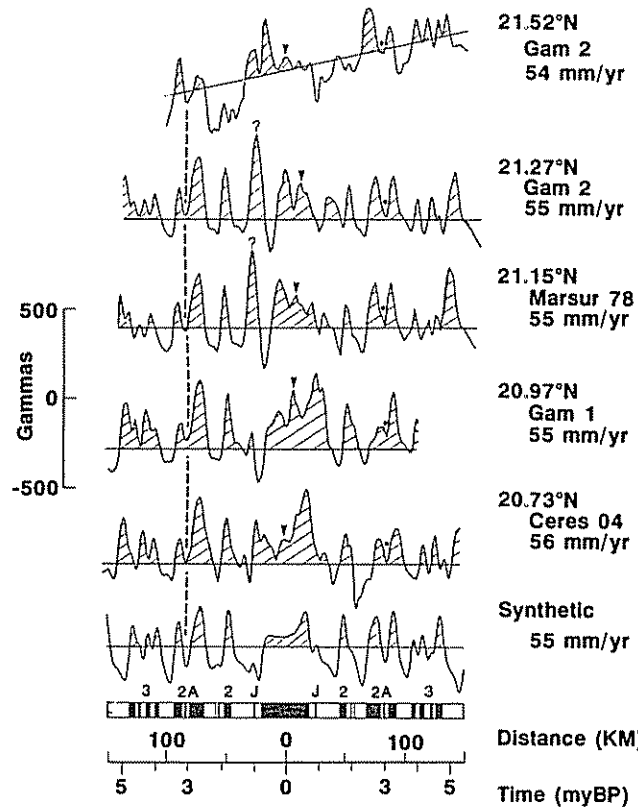

Fig. 4. Magnetic profiles along the southern Pacific–Rivera rise. The profiles, which are projected onto the N70°W, are typical of the best profiles along the rise. Comparison with the 55 mm yr^{-1} synthetic profile (bottom) suggests a southward increasing rate. The center of anomaly 2A northwest of the rise is aligned; the center of anomaly 2A southeast of the rise is marked by a small dot. The rise crest, as identified from the axial magnetic high and bathymetry, is marked by an arrow. The slope in the Gam 2 profile does not affect the anomaly correlations or the inferred spreading rate. Left to right represents northwest to southeast.

and an average N20°E trend for anomaly 2A, is only 36°. Thus the anomalies are nearly symmetric and are easy to identify. To check the accuracy of the anomaly correlations and spreading rates determined from the original data, we reduced two magnetic profiles to the pole by the computed 36° skewness and recorrelated them. The correlations and best fitting spreading rates are identical to those determined from the original data. We also determined spreading rates that best fit anomaly 2 (1.7 Ma) and the central (Brunhes) anomaly (0.7 Ma). The resulting sequence of post-3 Ma spreading rates permits us to assess the magnitude of any post-3 Ma spreading accelerations.

The Pacific–Rivera direction is given by four measurements of Rivera transform azimuths and 18 earthquake slip vectors, all located west of 106.25°W (Table 2). The N61°W trend measured from a compilation of bathymetric data along the western Rivera transform [*Dauphin and Ness*, 1990] agrees well with trends determined by *Sharman et al.* [1976] and *Larson* [1972] from older bathymetric maps. East of 107.5°W, Seabeam data define bathymetric lineations that may accommodate slip [*Bourgois et al.*, 1988*a*]. We measured three fault trends from the Seabeam data and assigned uncertainties based on a subjective assessment of the linearity and length of the fault, and the ease with which we could distinguish it from surrounding seafloor features. The typical measurement uncertainty associated with these lineations is 3°–5°.

Earthquake focal mechanisms used to determine the Pacific–Rivera direction are chosen using the following criteria: (1) The earthquake is strike-slip. (2) The focal mechanism is well constrained by first motion or body wave data. (3) The earthquake is located along the Rivera transform fault. Earthquakes 3–5 are omitted because they occur near short rise offsets where deformation may be more complex than simple strike-slip motion [*Macdonald et al.*, 1980; *Lonsdale*, 1989]. Earthquakes 6–9A are omitted because of their proximity to the ridge-transform intersection, where local deviations from transform-parallel slip may occur [*Fox and Gallo*, 1984; *Engeln et al.*, 1986]. Earthquake 10 is omitted because it is a normal faulting event. Earthquakes 28–31 and 34–35 are omitted because they occur east of the region where we are confident that Pacific–Rivera motion occurs (Figure 1).

Test for a Distinct Rivera Plate

We first tested whether the Rivera plate is a southward oceanic extension of North America or a northward salient of the Cocos plate. Such a test is practical and useful for two

reasons. First, data from the Pacific–Rivera rise and Rivera transform are now numerous and accurate enough to make a strong test. Second, estimates of the present-day rates of Pacific–North America and Pacific–Cocos motion differ significantly from those used in previous studies. Five magnetic profiles from the Gulf of California give a 3.0-m.y.-average Pacific–North America spreading rate of 48 mm yr^{-1} [*DeMets et al.*, 1987], 10 mm yr^{-1} slower than previous estimates, but consistent with the 49-50 mm yr^{-1} Pacific–North America rate required by global plate circuit closures [*DeMets et al.*, 1990] and very long baseline interferometry measurements [*Clark et al.*, 1987; *Argus and Gordon*, 1990; *Ward*, 1990]. Pacific–Cocos motion estimated from 25 magnetic profiles crossing the Pacific–Cocos rise and the NUVEL-1 Pacific–Cocos Euler vector is 10 mm yr^{-1} systematically slower than given by previous global plate motion models [*Chase*, 1978; *Minster and Jordan*, 1978].

Prior analyses that tested for an independent Rivera plate by comparing Pacific–Rivera rates and azimuths to Pacific–North America rates and azimuths from the Gulf of California reached a variety of conclusions. *Atwater* [1970] and *Larson* [1972] concluded that the Rivera plate moves with North America, but *Molnar* [1973] concluded that the Rivera plate is separate from North America. *Sharman et al* [1976] suggested that the Gulf of California and Rivera transform azimuths are too scattered to resolve a separate Rivera plate. *Minster and Jordan* [1979] and *Eissler and McNally* [1984] assumed that the Rivera plate is kinematically independent because of the 8–10 mm yr^{-1} difference between Pacific–Rivera rates just south of the Tamayo transform and the 58 mm yr^{-1} RM2 Pacific–North America rate they used for the southern Gulf of California [*Minster and Jordan*, 1978].

We compared the observed rates and azimuths along the Pacific–Rivera rise and Rivera transform to those predicted by the NUVEL-1 Pacific–North America and Pacific–Cocos Euler vectors (Figure 5). Because data from the Pacific–Rivera rise and Rivera transform were not used to derive the NUVEL-1 model, the NUVEL-1 Pacific–North America and Pacific–Cocos Euler vectors give unbiased predictions for this test. If the Rivera plate is part of North America, the Pacific–North America Euler vector should fit the Pacific–Rivera data nearly as well as the Pacific–Rivera best fitting vector, which is derived by minimizing the weighted, least squares misfit to Pacific–Rivera rise and Rivera transform data (Table 2) using fitting functions described by *DeMets et al.* [1990]. Similarly, if the Rivera plate is part of the Cocos plate, the rates and directions predicted by the Pacific–Cocos Euler vector should fit the Pacific–Rivera rise spreading rates and Rivera transform data. We find instead that Pacific–Rivera rates and azimuths differ systematically from those predicted by both the NUVEL-1 Pacific–North America and Pacific–Cocos Euler vectors (Figure 5). These systematic misfits are strong evidence for a distinct Rivera plate. The Pacific–North America and Pacific–Cocos Euler vectors misfit the three eastern Rivera transform fault azimuths measured from Seabeam data by 3–5 times their estimated uncertainties, and systematically misfit the earthquake slip vectors.

We tested the statistical significance of these misfits using the F-ratio test for an additional plate [*Stein and Gordon*, 1984]. Here, the F-ratio test determines whether the improved fit of the Pacific–Rivera best fitting vector relative to fits of the Pacific–North America or Pacific–Cocos Euler vectors exceeds that expected solely because the three model parameters that describe the best fitting vector are permitted to vary so as to minimize the total weighted least squares misfit to the data. The weighted least squares misfit to a datum is defined as the square of the difference between a predicted and observed rate or azimuth divided by the assigned uncertainty. The F-ratio test takes the form

$$F = \frac{(\chi^2_{alt} - \chi^2_{bfv}) / 3}{\chi^2_{bfv} / (N - 3)} \quad (1)$$

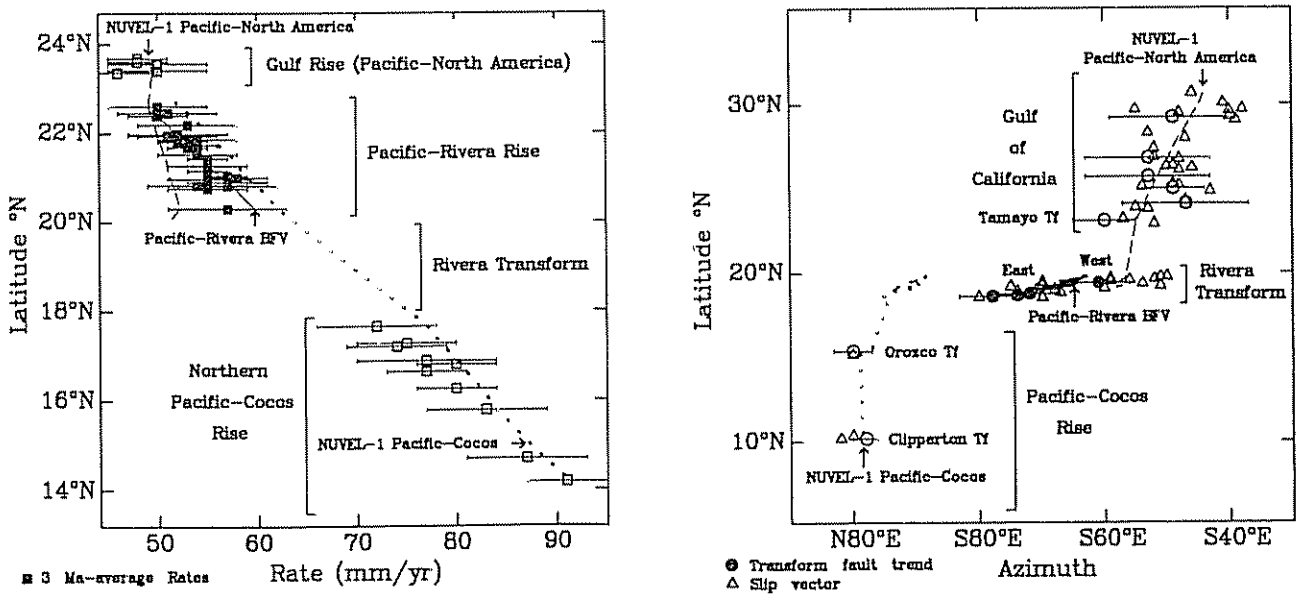

Fig. 5. Plate motion data from the Gulf of California, Pacific–Rivera rise, Rivera transform, and northern Pacific–Cocos rise compared to rates and azimuths predicted by the NUVEL-1 Pacific–North America and Pacific–Cocos Euler vectors. Pacific–Rivera rates (upper) and azimuths (lower) are systematically misfit by predictions of the Pacific–North America (dashes) and Pacific–Cocos (dotted line) Euler vectors, suggesting the Rivera plate is distinct from North America and Cocos.

where χ^2_{alt} is the least squares misfit of an alternative model (e.g., the Pacific–North America or Pacific–Cocos Euler vector) to the Pacific–Rivera data, χ^2_{bfv} is the least squares misfit of the Pacific–Rivera best fitting vector, and N is the number of Pacific–Rivera data. Values of F that exceed those computed for the 95% or 99% confidence levels indicate that data along the Pacific–Rivera rise and Rivera transform do not record motion of the Pacific plate relative to North America or Cocos. We use the F-ratio test instead of a chi-square test because the F-ratio test is insensitive to systematic overestimates or underestimates of errors in the data.

A comparison of the fit of the NUVEL-1 Pacific–North America Euler vector to that of the Pacific–Rivera best fitting vector using equation (1) gives $F = 193$. A similar comparison using the NUVEL-1 Pacific–Cocos Euler vector gives $F = 395$, significantly higher than the 99% confidence level in both cases ($F_{3,44;0.01} = 4.3$). The large values of F are attributable to the factor of 10 and greater increase in the reduced chi-square χ^2_ν, where $\chi^2_\nu = \chi^2/(N-3)$, of the alternative models relative to χ^2_ν for the Pacific–Rivera best fitting vector. We thus conclude that data along the Pacific–Rivera rise and the Rivera transform do not record Pacific–North America or Pacific–Cocos motion, and the Rivera plate is tectonically distinct.

A statistical test for an independent Rivera plate using the NUVEL-1 Pacific–North America and Pacific–Cocos Euler vectors is a strong test because the NUVEL-1 Euler vectors are derived from data from around the world and satisfy the redundant closure requirements in a global plate circuit. As a result, they are typically more accurate than Euler vectors determined from isolated data sets. Any systematic biases attributable to circuit nonclosures or errors in data collection and processing are minimized through the least squares adjustment. Systematic misfits of NUVEL-1 to the data used to derive the model are everywhere less than 2–3 mm yr^{-1} and 2°–5° [*DeMets et al.*, 1990], which suggests that any systematic biases, unless they pervade data from entire ocean basins or classes of plate boundaries, are small.

Kinematic Model

Although no data that unambiguously record Rivera–North America or Rivera–Cocos motion are available, Rivera plate motions relative to North America and Cocos are predicted by summing the Rivera–Pacific 3.0-m.y.-average Euler vector with the NUVEL-1 Pacific–North America and Pacific–Cocos 3.0-m.y.-average Euler vectors. Rivera plate Euler vectors and the uncertainties derived from the model covariances are listed in Table 3. The Pacific–Rivera covariance matrix is given in Table 4. Each of the 3.0-m.y.-average Euler vectors listed in Table 3 is consistent with closure constraints in the NUVEL-1 model.

The Pacific–Rivera best fitting vector fits the Pacific–Rivera data well, although the fit to the Rivera transform azimuthal data is somewhat problematic (Figure 6). For the best fitting vector, χ^2_ν is 0.16, comparable to χ^2_ν observed for the best fits to spreading ridge data in the NUVEL-1 data set. The low value of χ^2_ν suggests that the assigned data uncertainties have been overestimated by a factor of 3, resulting in standard model uncertainties that are comparable to 2–3σ uncertainties. The *Minster and Jordan* [1979] Pacific–Rivera Euler vector misfits the trend of the 3.0-m.y.-average rates and differs from the best fitting vector (Figure 6). The difference between the best fitting Pacific–Rivera Euler vector and that of the *Minster and Jordan* [1979] Euler vector is significant: $F = 48$, well above the 99% threshold of $F_{3,44;0.01}$=4.3.

As shown in Figure 6, the fit to the north-to-south gradient in Pacific–Rivera rise spreading rates is better than the fit to the Rivera transform azimuths. The best fitting vector fits the three Seabeam-derived fault trends east of 108.3°W, but systematically misfits azimuths west of 108.3°W. There are several plausible explanations for the systematic misfit. One possibility is that the tectonics of the Rivera plate have changed since 3.0 Ma. If so, the 3.0-m.y.-average rates are incompatible with the azimuthal data, which probably average over a shorter time interval. The transfer of spreading from

TABLE 3. Model Euler Vectors

Plate Pair	Latitude, °N	Longitude, °E	ω, deg–m.y.$^{-1}$	Error Ellipse σ_{max}	Error Ellipse σ_{min}	Error Ellipse ζ_{max}	σ_ω, deg–m.y.$^{-1}$
3.0-m.y.-Average Euler Vectors							
Rivera–Pacific	31.0	-102.4	2.562	3.6	0.6	21	0.596
Rivera–North America	22.8	-109.4	1.883	1.8	0.6	-57	0.607
Rivera–Cocos	6.7	-83.6	0.565	38.8	1.8	-56	0.48
1.7-m.y.-Average Euler Vector							
Rivera–Pacific	29.8	-102.9	2.918	1.9	0.5	22	0.399
0.7-m.y.-Average Euler Vectors							
Rivera–Pacific	27.9	-103.8	3.986	1.2	0.4	21	0.433
Rivera–North America	22.6	-108.0	3.32	0.7	0.4	-45	0.44

The first plate moves counterclockwise relative to the second plate. σ_{MAX} and σ_{MIN} are the angular lengths of the semi major and semi minor axes of the standard error region derived from the model covariances. ζ_{MAX} is the orientation of the major axis in degrees. The rotation rate uncertainty is determined from a one-dimensional marginal distribution, whereas the lengths of the principal axes are determined from a two-dimensional marginal distribution.

TABLE 4. Rivera–Pacific Variance-Covariance Matrix (Cartesian Pacific-Fixed Coordinates)

	x	y	z
x	80364	267302	-106199
y	267302	900297	-356095
z	-106199	-356095	141177

Units are 10^{-10} rad^2/m.y.^{2} Rows and columns are listed in the following order of components: x (0°N, 0°E), y (0°N, 90°E), z (90°N).

the Mathematician rise to the Pacific–Cocos rise [*Mammerickx*, 1984] that was completed shortly before 3.0 Ma more than doubled the length of the Rivera transform and transferred roughly half of the area of the Rivera plate that was subducting along the northern Middle America trench to the Cocos plate. The Rivera transform and the other boundaries of the Rivera plate probably evolved in response to the reorganization. Multi-beam mapping of other Pacific basin transforms [e.g., *Macdonald et al.*, 1979; *Searle*, 1983; *Madsen et al.*, 1986] indicates that transforms evolve on time scales of 1 m.y. or less. The present-day Pacific–Rivera slip direction could thus differ from the 3.0-m.y.-average direction by several degrees. When 0.7-m.y.-average spreading rates, which have a steeper north-to-south gradient than the 3.0-m.y.-average rates, are inverted with the Rivera transform data, the 0.7-m.y.-average best fitting vector fits the Rivera transform azimuths better than the 3.0-m.y.-average model (Figure 6). The shallow gradient in the 3.0-m.y.-average rates forces the Euler pole too far from the Rivera transform to permit a good fit to the azimuths, which change rapidly along the transform. Thus at least some of the azimuthal misfit is caused by a time-averaging discrepancy between the rate and directional data. Some of the misfit may go away once fault trends in the western Rivera transform valley are determined through swath mapping. A 3°–4° revision in the trend of the western part of the transform would resolve the entire discrepancy between the transform azimuths on the east and west ends of the transform, although it would fail to explain why earthquake slip vectors

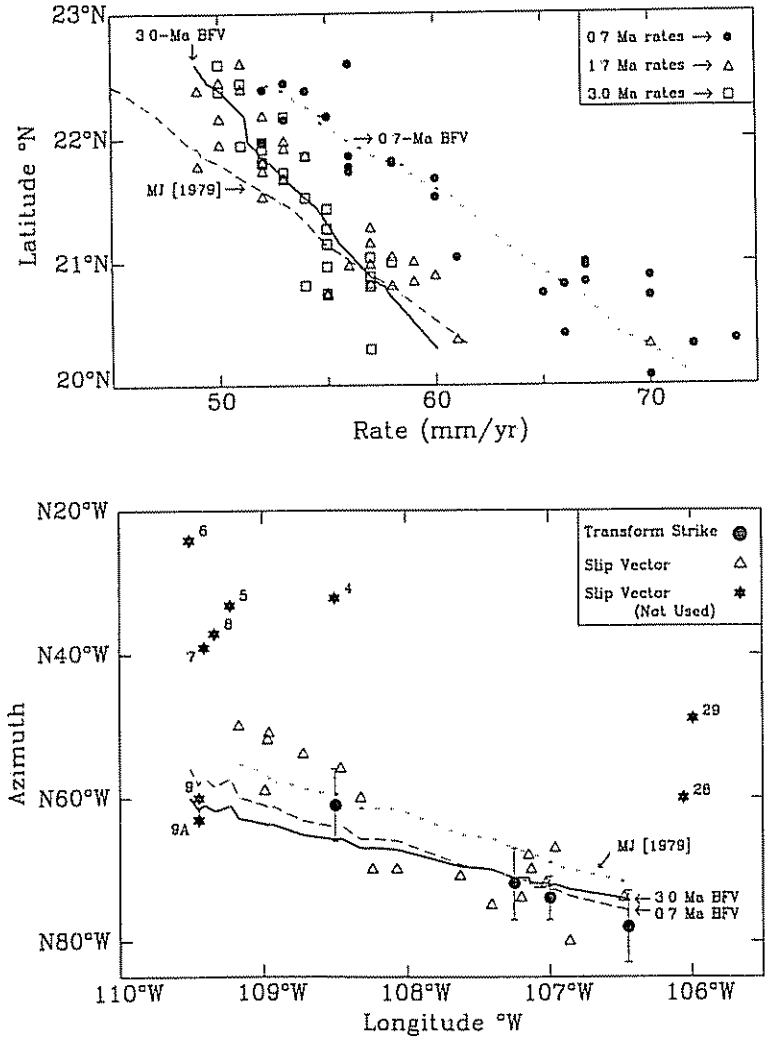

Fig. 6. Rates along the Pacific–Rivera rise and azimuths along the Rivera transform compared with rates and azimuths given by 3.0-m.y.-average and 0.7-m.y.-average Pacific–Rivera best fitting Euler vectors and the Euler vector determined by *Minster and Jordan* [1979] (MJ [1979]). The upper diagram compares rates averaged over the width of the central anomaly (0.7 Ma), anomaly 2 (1.7 Ma), and anomaly 2A (3.0 Ma). The *Minster and Jordan* [1979] Euler vector systematically misfits both sets of rates. Slip vectors 4–9A and 28–29 were not used to determine Pacific–Rivera motion.

along the western part of the transform are systematically misfit. A final possible explanation for the systematic misfit is that some of the lithosphere bordering parts of the Rivera transform valley may be deforming and the transform cannot be treated as a discrete Pacific–Rivera boundary. This possibility is suggested by the multiple subparallel valleys and apparent diffuse seismicity along much of the transform.

Because of the possibilities that some or all of the Rivera transform fault may not be a discrete Pacific–Rivera boundary, that time-averaging problems may affect our 3.0-m.y.-average model, and that incomplete mapping of the western Rivera transform may give a Pacific–Rivera direction several degrees different from the true slip direction, the formal uncertainties derived from inversion of the 3.0-m.y.-average data may be too small. The following discussion of Rivera–North America and Rivera–Cocos motion thus includes consideration of several alternative models, including 1.7-m.y.-average and 0.7-m.y.-average models.

Model Predictions

Rivera–North America

The Rivera–North America Euler vector derived here requires nearly orthogonal convergence varying from 6 mm yr^{-1} along the eastern Tamayo fracture zone to 20 mm yr^{-1} along the southern Acapulco trench (Figure 7). If subduction along the Acapulco trench had ceased in the past few million years, the predicted convergence between Rivera and North America would have to be accommodated elsewhere, possibly within the Rivera plate or within southwestern Mexico. Since no such deformation has been observed, it seems likely that convergence occurs as slow subduction along the Acapulco trench and possibly as underthrusting beneath the Tres Marias islands and escarpment. Although there is presently much less seismicity along the Acapulco trench than along the Middle America trench to the south where the Cocos plate is subduct-

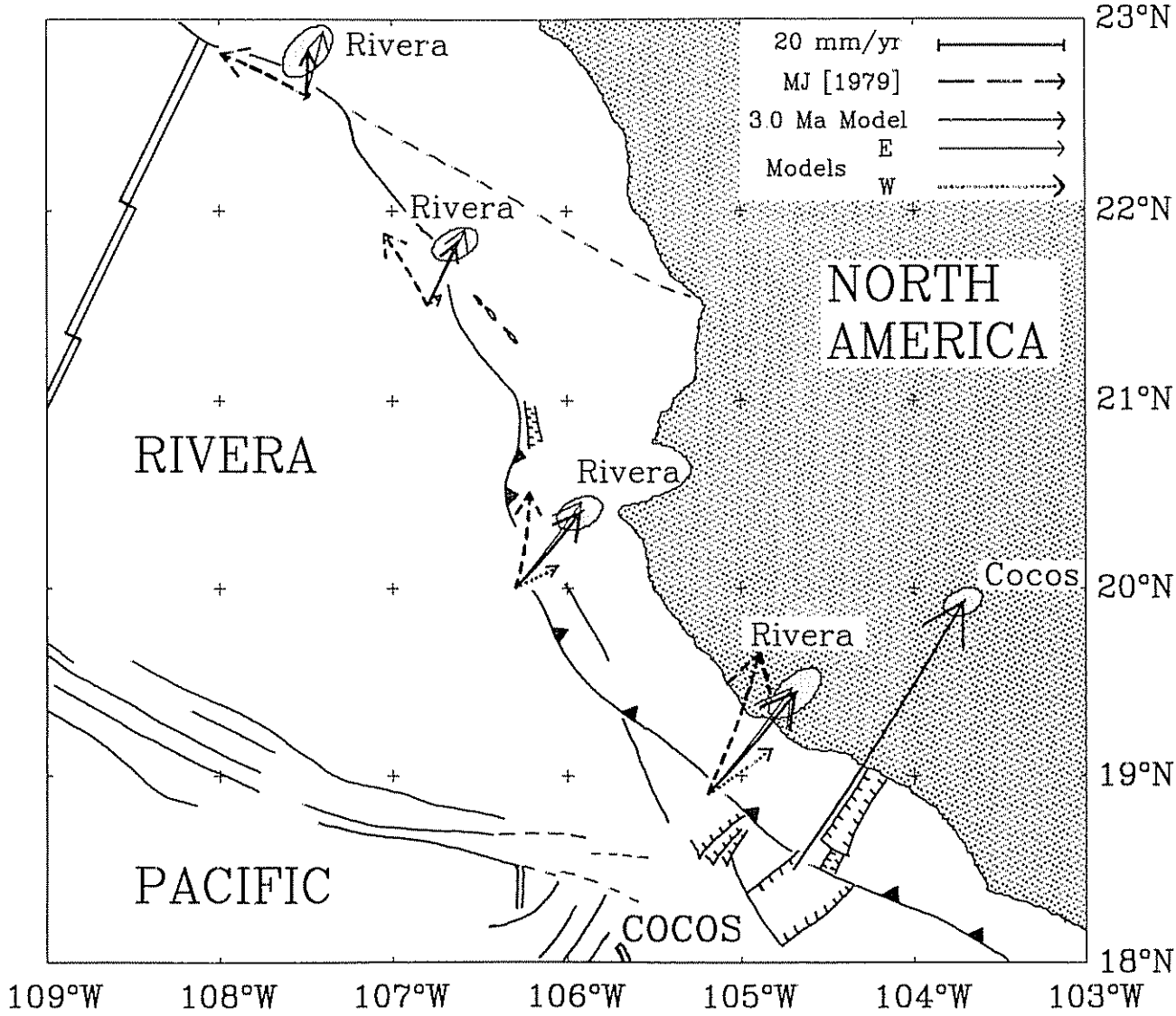

Fig. 7. Rivera–North America and Cocos–North America linear velocity vectors predicted by 3.0-m.y.-average Euler vectors (Table 3). Arrows show velocity predictions at the origin of each vector, and the standard error ellipses represent the two-dimensional velocity uncertainties extracted from the model covariances. Rivera–North America velocities are shown for four models, the 3.0-m.y.-average model, the *Minster and Jordan* [1979] model, and models E and W, which are discussed in the text. The *Minster and Jordan* [1979] model predicts motion significantly counterclockwise from that predicted by the models derived here.

ing, the low level of seismicity need not preclude subduction; there is also little seismicity along the southern Chile trench, where subduction occurs at a similar ~20 mm yr^{-1} rate.

To examine how uncertainties about the present-day slip direction along the Rivera transform affect the Rivera–North America velocities predicted from closure of the Pacific–Rivera–North America plate circuit, we tested two end-member models for the behavior of the Rivera transform. In one case (model W), we assumed that only the azimuths located west of 108.3°W accurately record the 3.0-m.y.-average Pacific–Rivera direction; in the other case (model E), we used azimuths from east of 108.3°W to constrain the 3.0-m.y.-average Pacific–Rivera direction. For model E, we found that Rivera–North America velocities along most of the boundary were similar to those of the preferred 3.0-m.y.-average model. For model W, Rivera–North America velocities were a few degrees clockwise and 50% or more slower than the preferred 3.0-m.y.-average model. Model W suggests that convergence along nearly the entire boundary north of the Acapulco trench is negligible. This analysis demonstrates that estimates of the Rivera–North America velocities depend critically on what we assume about motion along the Rivera transform. Small changes in the Rivera–North America Euler pole, which is located close to the Rivera plate, give large changes in the predicted Rivera–North America velocities.

The 3.0-m.y.-average model and models E and W all give velocities slower than and clockwise from those predicted by the *Minster and Jordan* [1979] model (Figure 7). At 19.4°N, 105.0°W, near the only earthquake mechanism (32) that appears to record Rivera–North America subduction, the predicted convergence of 19±3 mm yr^{-1} directed N40°E±5° is consistent with the N36°E slip direction from this earthquake mechanism (Figure 1). (The quoted uncertainties are 1σ and are determined through linear propagation of errors using the full covariance matrix.) The predicted motion differs from the 22 mm yr^{-1}, N19°E velocity predicted by *Minster and Jordan* [1979]. At 21.5°N, 106.8°W, along the Tres Marias escarpment, the predicted velocity of 10±3 mm yr^{-1}, N29°E±9° is nearly normal to the escarpment and is 54° clockwise from the 12 mm yr^{-1}, N25°W velocity predicted by *Minster and Jordan* [1979]. Earthquake 2 (Figure 1) [*Goff et al.*, 1987] gives a convergence direction (N02°E) midway between the predictions of the two models.

At 22.6°N, 107.5°W, near the eastern Tamayo fracture zone, the predicted velocity is 6±3 mm yr^{-1} directed N7°E±22°, 8 mm yr^{-1} slower than and 66° clockwise from the 14 mm yr^{-1}, N59°W velocity predicted by *Minster and Jordan* [1979]. Neither of the small earthquakes near 22.5°N, 107°W (1 and 2A) unambiguously supports either model.

Given that the Pacific–Rivera half-spreading rate exceeds the Rivera–North America convergence rate, the Rivera plate is not subducting into extinction, as did other fragments of the Farallon plate. The increase in the area of the Rivera plate from Pacific–Rivera spreading (~9700 km^2/m.y.) exceeds the area lost to subduction along the Acapulco trench (~6600 km^2/m.y.). Interestingly, the Rivera–North America convergence rate along the Rivera–North America plate boundary decreases more rapidly to the north than does the Pacific–Rivera spreading rate, suggesting that the net accretion rate increases to the north.

Rivera–Cocos

The Cocos–Rivera Euler vector predicts 29±4 mm yr^{-1}, N30°E±5° motion of the Cocos plate relative to a fixed Rivera plate at 18.6°N, 105.2°W. At the same location, the *Eissler and McNally* [1984] and *Bandy and Yan* [1989] models for Rivera–Cocos motion predict motion of 29 mm yr^{-1}, N51°E, and 21 mm yr^{-1}, N13°E, respectively. Depending on the orientation of the seafloor structures that accommodate Rivera–Cocos motion, sinistral strike-slip, convergence, or some combination of the two would be expected given the predicted velocity. As noted by *Eissler and McNally* [1984], two strike-slip earthquakes (30 and 31) may record deformation between the two plates. It is unclear how and where convergence might be accommodated, and the relationship of the two seafloor grabens that extend west from the trench near where the Rivera and Cocos plates may intersect (Figures 1 and 7) to any convergent or strike-slip motion is also unclear.

Time Variable Pacific–Rivera Motion and Implications for Rivera–North America Kinematics

To examine possible time variations in Pacific–Rivera motion, we also determined spreading rates averaged over the past 1.7 m.y. and 700,000 years (Figure 6). The 0.7-m.y.-average rates are 10–20% faster than the 3.0-m.y.-average rates, but the 1.7-m.y.-average rates are only marginally faster. The three sets of rates suggest that the Pacific–Rivera Euler vector has migrated closer to the Rivera plate since 3.0 Ma and the spreading gradient has correspondingly increased (Table 3). A recent determination of Rivera–Pacific motion since 1 Ma predicts rates and directions within 2 mm yr^{-1} and 3° of those predicted by our model [*Bandy and Yan*, 1989]. The post-3 Ma change in spreading rates and the migration of the Pacific–Rivera Euler vector suggest that Rivera plate kinematics are still evolving, probably in response to the ~3.4 Ma cessation of spreading along the Mathematician rise that established the Rivera transform as the southern boundary of the Rivera plate [*Mammerickx and Klitgord*, 1982; *Mammerickx et al.*, 1988].

If Pacific–North America motion has remained relatively constant over the past 3 m.y., then a post-3 Ma increase in the Pacific–Rivera spreading rate implies a corresponding increase in the Rivera–North America convergence rate. Pacific–North America Euler vectors derived from very long baseline interferometric measurements between 1983 and 1987 differ little from the NUVEL-1 Pacific–North America Euler vector, suggesting that Pacific–North America motion has changed little since 3 Ma [*Argus and Gordon*, 1990; *Ward*, 1990]. Given that Pacific–North America motion appears to have changed little since 3 Ma, we constructed a Rivera–North America 0.7-m.y.-average model by combining the 0.7-m.y.-average Pacific–Rivera Euler vector (Table 3) with the NUVEL-1 Pacific–North America Euler vector. As expected, velocities predicted by the 0.7-m.y.-average Rivera–North America model are faster than and clockwise from those predicted by the 3.0-m.y.-average model. For instance, at 18.9°N, 105.2°W, the 0.7-m.y.-average model predicts motion of 29±3 mm yr^{-1}, N55±4°E, 9 mm yr^{-1} faster than and 10° clockwise from motion predicted by the 3.0-m.y.-average model. These results suggest that subduction along the Acapulco trench may be up to 50% faster than given by the 3.0-m.y.-average model. A better estimate of the Rivera–North America convergence rate since 0.7 Ma requires either a more accurate estimate of 0.7-m.y.-average Pacific–North America motion or geodetic measurements to markers anchored on Rivera seafloor.

Earthquake Repeat Times in the Jalisco Region

An accurate description of Rivera–North America motion is necessary for estimating earthquake recurrence intervals in the Jalisco region, where historic data suggest occasional large earthquakes [*McNally and Minster*, 1981; *Astiz and Kanamori*, 1984; *Eissler and McNally*, 1984; *Singh et al.*, 1985; *Anderson et al.* 1989]. *Singh et al.* [1985] estimate a recurrence period of 77 years for a convergence rate of 20 mm yr^{-1} along the Acapulco trench, similar to the 70–100 year interval derived from the 19±3 mm yr^{-1} convergence rate predicted by the 3.0-m.y.-average model at 19.4°N, 105°W. For the 27±5 mm yr^{-1} convergence rate predicted by the 0.7-m.y.-average Rivera–North America model at 19.4°N, 105°W, the recurrence interval becomes 48–70 years, close to the present interval of seismic quiescence. However, given the uncertainties about the nature of slip along the Rivera transform discussed above, the 155 cm of seismic slip released in the 1932 earthquakes [*Singh et al.*, 1985] could take as long as 130 years to accumulate. Time variable plate motion, an unknown amount of aseismic slip in the subduction zone, and our present state of knowledge about the Rivera transform kinematics lend considerable uncertainty to our estimate of the recurrence interval for the Jalisco region.

Oblique Subduction Along the Middle America Trench and Implications for Deformation in Mexico

In the remainder of the paper, we discuss the hypothesis that oblique subduction of the Cocos plate causes slivers of southwestern Mexico to move several mm yr^{-1} toward the southeast relative to stable North America. We present several lines of evidence that suggest that opening along the Colima rift and slip along the Trans-Mexican Volcanic Belt and Chapala-Oaxaca fault zone are consistent with such a model. This hypothesis originates in geologic, seismologic, paleomagnetic, and plate motion studies that indicate that oblique subduction commonly causes rotations and trench-parallel translations of crustal blocks that are trapped between a subducting oceanic plate and the stable interior of an overlying plate [*Fitch*, 1972; *Seno*, 1985; *Beck*, 1986; *Beck et al.*, 1986; *Jarrard*, 1986; *Geist et al.*, 1988; *DeMets et al.*, 1990]. Because block rotations and translations result in divergence and convergence at the trailing and leading edges of crustal blocks, deformation consisting of extension (pull-apart basins or rifts), compression, and strike-slip faulting is to be expected inboard from trenches where subduction is oblique.

A model for deformation in southwestern Mexico should include the subducting Rivera and Cocos plates, the Jalisco block, which overlies subducted Rivera plate, the Michoacan and Guerrero blocks, which overly the subducting Cocos plate, and the North American plate (Figure 8). Four principal zones of deformation, the Tepic-Chapala rift, the Colima rift, the Chapala-Oaxaca fault zone, and the Trans-Mexican Volcanic Belt, which includes the Chapala rift and Chapala-Tula fault zone (Figure 1), separate the Jalisco, Michoacan, and Guerrero blocks, and North American plate. Too few observations exist to present a unique kinematic model for the motions of these blocks. We thus focus on using rigid-plate constraints imposed by the NUVEL-1 model for Cocos–North America motion to estimate the maximum present-day rate of deformation within western Mexico. We demonstrate that the predicted rate and direction of present-day deformation are consistent with geologic observations of Plio-Pleistocene deformation along the Trans-Mexican Volcanic Belt, the Chapala-Oaxaca fault zone, and the Colima rift.

Geologic and Seismologic Evidence for Southeastward Motion of the Guerrero and Michoacan Blocks

The N33°E±1° Cocos–North America convergence direction given by NUVEL-1 along the northern Middle America trench is 12° clockwise from the N22°E±2° direction normal to the trench. *Jarrard* [1986] observes that oblique convergence along trenches is commonly partitioned into subduction nearly normal to the trench and along-trench translation of slivers of the overriding plate. Given the observed clockwise sense of obliquity, post-3 Ma sinistral displacements and/or counterclockwise rotations of the Michoacan and/or Guerrero blocks relative to North America might then be expected.

Geologic data along two fault systems in western Mexico are consistent with southeastward motion of parts of southwestern Mexico relative to North America in the past few m.y. *Harrison and Johnson* [1988] infer sinistral slip along the trench-parallel Chapala-Oaxaca fault zone and the east-west trending Chapala-Tula fault zone, which coincides along much of its length with the Trans-Mexican Volcanic Belt, a continental volcanic arc probably related to the subduction of the Cocos plate beneath North America [*Molnar and Sykes*, 1969; *Nixon*, 1982; *Suarez and Singh*, 1986] (Figures 1 and 8). The Chapala-Oaxaca fault zone, a 700-km-long system of trench-parallel faults and fractures southeast of the Colima rift, is well defined by structures interpreted from Landsat Thematic Mapper imagery, and appears to have accommodated several kilometers of sinistral slip since 5 Ma [*Harrison and Johnson*, 1988]. Along the Chapala-Tula fault zone, the alignment of north dipping, right stepping en echelon normal faults that cut Plio-Quaternary volcanic deposits is consistent with active transtension with a sinistral component. *Pasquarè et al* [1988] infer sinistral shear, though in a more E-W direction than Harrison and Johnson, along the central sector of the Trans-Mexican Volcanic Belt from structural analyses of folds, faults, lineaments, and cleavages in Early-Late Pleistocene rocks.

If, as the evidence suggests, sinistral slip occurs along either or both of these fault systems, then earthquake slip vectors from the northern Middle America trench record subduction of the Cocos plate beneath a coastal block that is moving relative to North America. A linear velocity vector triangle between the Cocos, North America, and a southeastward moving coastal block (Figure 8) suggests that earthquake slip vectors from the northern Middle America trench should trend systematically counterclockwise from the predicted Cocos–North America direction. As shown in Figure 8, the predicted counterclockwise bias is observed for slip vectors located west of 98°W. Thus the sense of obliquity predicted from the NUVEL-1 model, geologic evidence for recent deformation in southwestern Mexico, and slip vectors from the northern Middle America trench are all consistent with a model in which the Michoacan and Guerrero blocks are translating to the southeast relative to North America.

Present-Day Rate of Southeastward Slip

If we assume that the entire difference between the predicted Cocos–North America direction and the direction given by the trench slip vectors is caused by trench-parallel, sinistral translation of the Michoacan and Guerrero blocks, the

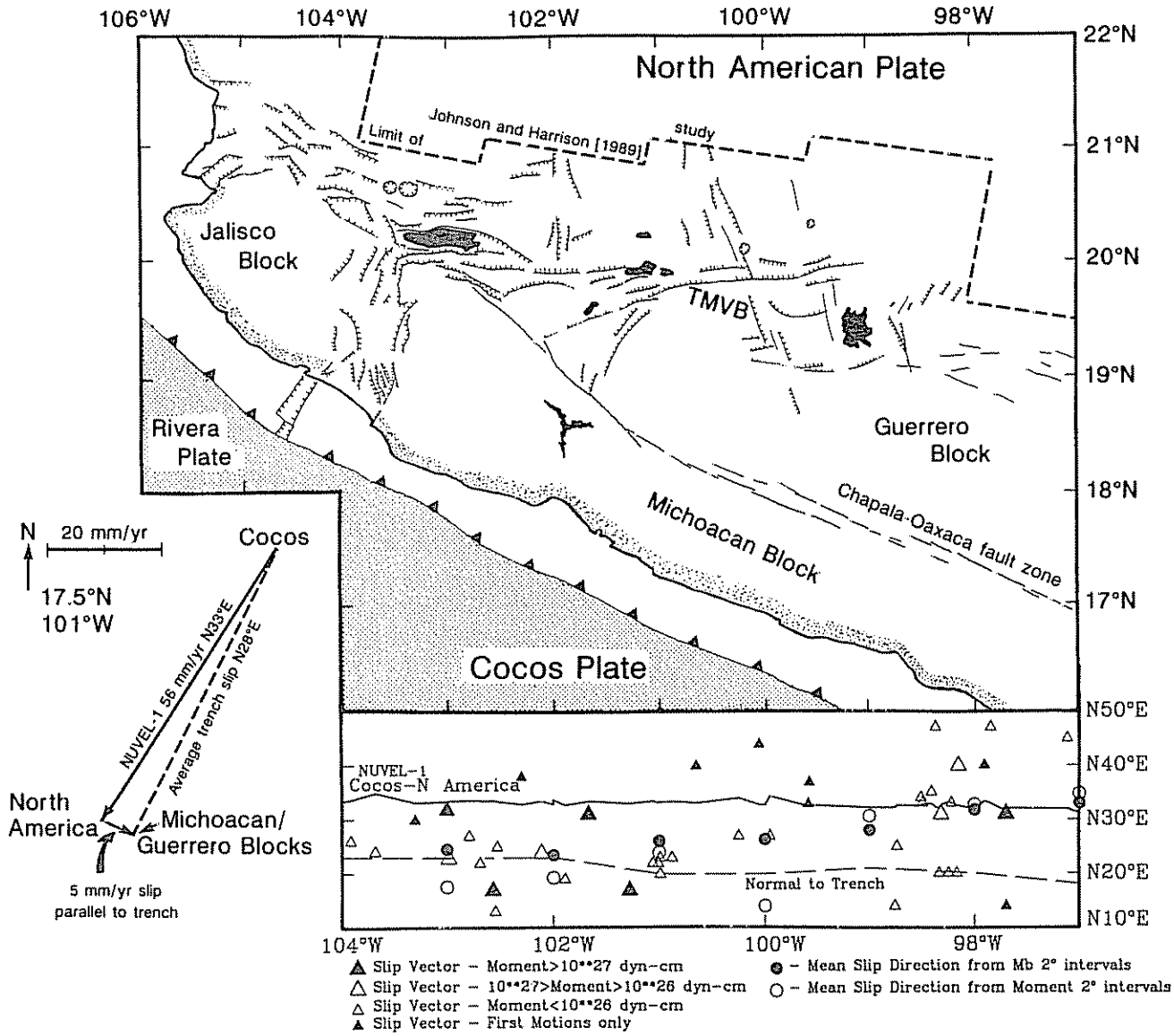

Fig. 8. Summary of evidence for southeastward motion of the Guerrero and/or Michoacan blocks of southwestern Mexico. Trench slip vectors from 104°W-97°W (below) are oriented between the trench-normal direction and the predicted Cocos–North America convergence direction. This bias is consistent with southeastward motion of western Mexico relative to the North American plate (lower left). Geometry of the Michoacan and Guerrero blocks adopted from *Harrison and Johnson* [1988]. Earthquake slip directions are derived from focal mechanisms given in *Molnar and Sykes* [1969], *Dean and Drake* [1978], *Chael and Stewart* [1982], *Burbach et al.* [1984], and Harvard centroid-moment tensor solutions.

rate of sinistral slip, V_s, can be determined using the relation (modified from *Jarrard* [1986])

$$V_s = V_c \sin(\theta) / \cos(\psi - \theta) \quad (2)$$

where V_c is the Cocos–North America convergence rate, θ is the angle between the predicted convergence direction and the direction given by trench slip vectors, and ψ is the angle between the predicted convergence direction and the direction normal to the trench. Slip along the Chapala-Oaxaca fault zone appears to parallel the trench; however, deformation along the Trans-Mexican Volcanic Belt may not be strictly trench-parallel. Any deviation from trench-parallel slip would result in a faster predicted rate of deformation. A more rigorous approach to the problem of estimating distributed deformation rates and directions is presented by *Minster and Jordan* [1984]. Too few geologic, geodetic, and seismologic data from this region are presently available for such an analysis.

To determine the mean direction given by trench slip vectors, we averaged slip directions from 50 earthquake mechanisms along the Middle America trench west of 95.8°W (Figure 8). Average directions are first computed by weighting individual slip vectors by the body-wave magnitude m_b of the earthquake; the analysis is then repeated using seismic moment. Each of the weighting schemes has shortcomings. Weighting slip vectors by body-wave magnitude probably underweights slip directions determined from the largest earthquakes, which release three to five orders of magnitude more energy than small earthquakes. Weighting by seismic moment, which is proportional to the area of fault rupture and amount of fault slip, corrects this problem, but introduces an additional one: it

is unlikely that slip directions determined from large earthquakes are three to five times more representative of the true convergence direction than those from small earthquakes. For instance, overweighting a slip vector from a large earthquake that has an anomalous subduction direction because it ruptures an along-trench heterogeneity such as a subducting seamount could bias the estimated mean convergence direction for a given segment along the trench by 10°–20°, particularly if only one or two large earthquakes are available for that segment. As seen in Figure 8, slip directions derived from small earthquakes are only slightly more scattered about the predicted convergence direction than directions from large earthquakes, which suggests that small and large earthquakes should be assigned more equitable weights until there are enough large earthquakes to achieve a meaningful average direction for each trench segment.

The mean subduction direction computed using body-wave magnitude weighting is N28°±2°E. The mean subduction direction computed using seismic moment weighting is N24°±2°E. At 17.5°N, 101°W, the Cocos–North America velocity predicted by the NUVEL-1 model is 56±2 mm yr^{-1} directed N33°E±1°, and the average trench-normal direction is N22°E±2°. The rate of trench-parallel deformation, V_s, computed from equation (2) is 5±2 mm yr^{-1} for weighting by m_b, and 9±2 mm yr^{-1} for weighting by seismic moment. Uncertainties for V_s were computed by linear propagation of errors for each of the quantities in equation (2).

The inferred rate of trench-parallel slip can vary be a factor of 2 or 3 with changes of only several degrees in the convergence direction estimated from trench earthquake slip vectors and in the predicted Cocos-North America direction. This suggests that the slip rate uncertainty estimated solely through linear propagation of errors is too small. Because estimates of the along-trench convergence direction are likely to change as future earthquakes supplement the small number of trench slip vectors presently available for most segments along the trench, and because the Cocos–North America direction predicted by NUVEL-1 is a 3.0-m.y.-average direction that could differ from the present-day direction by several degrees, we believe that this analysis demonstrates only that the plate kinematic data are consistent with sinistral trench-parallel motion of 0–10 mm yr^{-1}.

A model where western Mexico moves several mm yr^{-1} toward the southeast relative to North America, though consistent with geological and seismological observations, is nonunique, and the model and estimated slip rate are only simple first steps toward understanding deformation in Mexico. The model presented here gives no information about how slip is distributed along individual fault zones such as the Chapala-Oaxaca fault zone or the Trans-Mexican Volcanic Belt. Moreover, the mean Middle America trench slip directions appear to trend increasingly clockwise southeastward along the trench, and east of 98°W, they agree well with the predicted Cocos–North America direction. Because of the as-of-yet small sample of large subduction zone earthquakes, it is unclear whether the along-trench trend in mean slip directions has any geological significance. Regional geologic and geodetic studies are essential for answering many of these questions.

Motion of the Jalisco Block

Relating motion of the Jalisco block to oblique subduction of the Rivera plate, with its attendant implications for deformation along the Tepic-Chapala and Colima rifts, is difficult because the uncertainties in the predicted Rivera–North America convergence direction along the Acapulco trench are too large to determine with any confidence whether subduction is oblique to the continental margin. In a model where Jalisco block motion is driven by oblique subduction of the Rivera plate, we cannot therefore predict how the Jalisco block moves relative to North America. Geologic and geodetic measurements within the Tepic-Chapala rift suggest dextral strike-slip motion across the rift of 2 mm yr^{-1} [*Nieto-Obregon et al.*, 1985; *Allan et al.*, 1990]. In contrast, *Harrison and Johnson* [1988] suggest that the measured dextral slip is part of regional sinistral transtension along the rift.

Is the Colima Rift a Trailing Edge Pull-Apart Basin?

If the Michoacan block is moving toward the southeast at a rate of several mm yr^{-1}, extension must occur somewhere in the Jalisco region behind its trailing edge. We hypothesize that the Colima rift accommodates all or some of the extension predicted by the model discussed above. However, sustained rifting of even a few mm yr^{-1} over several million years would exceed the several kilometers of geologically observed extension along the northern Colima rift [*Allan*, 1986]. This suggests that either our estimate of 5–9 mm yr^{-1} of southeastward motion of the Michoacan and Guerrero blocks is too high, or that the predicted extension is distributed across a larger area that includes the Colima rift. The total rate of extension across the Colima rift depends on how fast the Michoacan block moves to the southeast and on the unknown velocity of the Jalisco block, which borders the rift to the northwest. Motion of Jalisco to the northwest, corresponding to dextral slip along the Tepic-Chapala rift, would increase the rate of Colima rifting; motion of Jalisco toward the southeast, corresponding to sinistral transtension across the Tepic-Chapala rift, would decrease the extension rate.

Nixon [1982] suggests that extension along the Colima rift may be related to interaction of the Cocos and Rivera plates along the subducted part of the Rivera fracture zone; however, in light of the complex post-10 Ma kinematic history of the northern Cocos, Rivera, and now extinct Mathematican plate [*Klitgord and Mammerickx*, 1982; *Mammerickx*, 1984; *Mammerickx et al.*, 1988], the suggestion that the Rivera fracture zone is subducting beneath the Colima rift may be incorrect and bears closer scrutiny.

Discussion

Luhr et al. [1985] suggest that the Tepic-Chapala, Chapala, and Colima rifts are the initial manifestations of an eastward jump of the Pacific–Rivera rise that will eventually transfer the Rivera plate and Jalisco region to the Pacific plate, much as Baja California was transferred to the Pacific plate. This intriguing hypothesis is difficult to test. Spreading rates along the Pacific–Rivera rise have increased since 3 Ma (Figure 6), contrary to the expectation that spreading along the Pacific–Rivera rise should slow as rifting is established onshore. It is even more unlikely that the Jalisco block is already part of the Rivera plate [*Bandy et al.*, 1988]. The 3.0-m.y.-average and 0.7-m.y.-average models presented here require 20 mm yr^{-1} or more of convergence between the Rivera and North American plates. If the Jalisco block were attached to the Rivera plate, the Tepic-Chapala rift would have

to accommodate convergence, which is not observed. Nonetheless, it is still unclear how deformation along the Tepic-Chapala rift is related to subduction of the Rivera plate north of 20°N, if it is at all. Uncertainties about the direction of Rivera plate convergence and about the present-day direction of slip along the Tepic-Chapala rift complicate any effort to construct a kinematic model. Geodetic measurements coupled with detailed field studies may offer the best opportunity for understanding the regional neotectonics.

The hypothesis presented here, that opening along the Colima rift is a response to southeastward translation of the Michoacan block that is being induced by oblique subduction of the Cocos plate, is appealing for several reasons. Oblique subduction is associated with present-day and past forearc deformation along other trenches. For instance, the San Andreas fault and rifting in the Gulf of California may have originated through oblique subduction of the Farallon plate beneath western California before 5 Ma [*Beck*, 1986]. Moreover, along much of the western margin of the Americas since 100 Ma, periods of oblique subduction appear to correlate with coastal transport of terranes and in situ block rotations against landward buttresses [*Beck et al.*, 1981; *Beck*, 1986, 1987]. Further study of rifting and strike-slip faulting in southwestern Mexico may offer useful insights into the relationship between onshore deformation and oblique subduction.

Acknowledgments. We thank Bill Bandy for helpful discussions and reprints despite the considerable overlap in our ongoing research. We also thank Jamie Allan, Gordon Ness, and Peter Lonsdale for helpful discussions, and Peter Molnar, Chris Harrison, and two anonymous reviewers for constructive comments. This work was initiated at the Naval Research Laboratory, and was sponsored by a National Research Council Research Associateship. The writing and publication were completed at the Jet Propulsion Laboratory, California Institute of Technology, under a contract with NASA. Reference herein to any specific commercial product, process, or service by trade name, trademark, manufacturer, or otherwise does not constitute or imply its endorsement by the U.S. government or the Jet Propulsion Laboratory, California Institute of Technology. This research was also supported by NSF grant EAR 8618038 and NASA grant NAG5-885.

REFERENCES

Allan, J. F., Geology of the northern Colima and Zacoalco grabens, southwest Mexico: Late Cenozoic rifting in the Mexican volcanic belt, *Geol. Soc. Am. Bull.*, *97*, 473–485, 1986.

Allan, J. F., S. A. Nelson, J. F. Luhr, I. E. S. Carmichael, and M. Wopat, Pliocene-recent rifting in southwest Mexico and associated alkaline volcanism, *Mem. Am. Assoc. Pet. Geol.*, *47*, in press, 1990.

Anderson, J. G., S. K. Singh, J. M. Espindola, and J. Yamamoto, Seismic strain release in the Mexican subduction thrust, *Phys. Earth Planet. Inter.*, *58*, 307–322, 1989.

Argus, D. F., and R. G. Gordon, Pacific–North American plate motion from very long baseline interferometry compared with motion inferred from magnetic anomalies, transform faults, and earthquake slip vectors, *J. Geophys. Res.*, *95*, 17,315–17,324, 1990.

Astiz, L., and H. Kanamori, An earthquake doublet in Ometepec, Guerrero, Mexico, *Phys. Earth Planet. Inter.*, *34*, 24–45, 1984.

Atwater, T., Implications of plate tectonics for the Cenozoic tectonic evolution of western North America, *Geol. Soc. Am. Bull.*, *81*, 3513–3536, 1970.

Bandy, W. L., and C-Y. Yan, Present-day Rivera–Pacific and Rivera–Cocos relative plate motions (abstract), *Eos Trans. AGU*, *70*, 1342, 1989.

Bandy, W., T. W. C. Hilde, and J. Bourgois, Redefinition of the plate boundaries between the Pacific, Rivera, Cocos, and North American plates at the north end of the Middle America trench (abstract), *Eos Trans. AGU*, *69*, 1415–1416, 1988.

Beck, M. E., Jr., Model for late Mesozoic-early Tertiary tectonics of coastal California and western Mexico and speculations on the origin of the San Andreas fault, *Tectonics*, *5*, 49–64, 1986.

Beck, M. E., Jr., Tectonic rotations on the leading edge of South America: The Bolovian orocline revisited, *Geology*, *15*, 806–808, 1987.

Beck, M. E., Jr., R. F. Burmester, D. C. Engebretson, and R. Schoonover, Northward translation of Mesozoic batholiths, western North America: Paleomagnetic evidence and tectonic significance, *Geofis. Inter.*, *20*, 143–162, 1981.

Beck, M. E., Jr., R. E. Drake, and R. F. Butler, Paleomagnetism of Cretaceous volcanic rocks from coastal Chile and implications for the tectonics of the Andes, *Geology*, *14*, 132–136, 1986.

Blakely, R., and A. Cox, Identification of short polarity events by transforming marine magnetic profiles to the pole, *J. Geophys. Res.*, *77*, 4339–4349, 1972.

Bourgois, J., V. Renard, J. Aubouin, W. Bandy, E. Barrier, T. Calmus, J. Carfantan, J. Guerrero, J. Mammerickx, B. Mercier de Lepinay, F. Michaud, and M. Sosson, La jonction orientale de la dorsale Est-Pacifique avec la zone de fracture de Rivera au large du Mexique, *C. R. Acad. Sci. Paris*, *307*, *Ser. II*, 617–626, 1988*a*.

Bourgois, J., V. Renard, J. Aubouin, W. Bandy, E. Barrier, T. Calmus, J. Carfantan, J. Guerrero, J. Mammerickx, B. Mercier de Lepinay, F. Michaud, and M. Sosson, Fragmentation en cours du bord Ouest du Continent Nord Américain: Les frontières sous-marines du Bloc Jalisco (Mexique), *C. R. Acad. Sci. Paris*, *307*, *Ser. II*, 1121–1130, 1988*b*.

Burbach, G., C. Frohlich, W. D. Pennington, and T. Matumoto, Seismicity and tectonics of the subducted Cocos plate, *J. Geophys. Res.*, *89*, 7719–7735, 1984.

Chael, E. P., and G. S. Stewart, Recent large earthquakes along the Middle American Trench and their implications for the subduction process, *J. Geophys. Res.*, *87*, 329–338, 1982.

Chase, C., Plate kinematics: The Americas, East Africa, and the rest of the world, *Earth Planet. Sci. Lett.*, *37*, 355–368, 1978.

Clark, T. A., D. Gordon, W. E. Himwich, C. Ma, A. Mallama, and J. W. Ryan, Determination of relative site motions in the western United States using Mark II very long baseline radio interferometry, *J. Geophys. Res.*, *92*, 12,741–12,750, 1987.

Coney, P. J., and S. J. Reynolds, Cordilleran Benioff zones, *Nature*, *270*, 403–406, 1977.

Cross, T. A., and R. H. Pilger, Jr., Constraints on absolute motion and plate interaction inferred from Cenozoic igneous activity in the western United States, *Am. J. Sci.*, *278*, 865–902, 1978.

Dauphin, J. P., and G. E. Ness, Bathymetry of the Gulf and Peninsular province of the Californias, *Mem. Am. Assoc. Pet. Geol.*, *47*, in press, 1990.

Dean, B. W., and D. L. Drake, Focal mechanism solutions and tectonics of the Middle America arc, *J. Geol.*, *86*, 111–128, 1978.

DeMets, C., R. G. Gordon, S. Stein, and D. F. Argus, A revised estimate of Pacific–North America motion and implications for western North America plate boundary zone tectonics, *Geophys. Res. Lett.*, *14*, 911–914, 1987.

DeMets, C., R. G. Gordon, D. F. Argus, and S. Stein, Current plate motions, *Geophys. J. Int.*, *101*, 425–478, 1990.

Dziewonski, A. M., and J. H. Woodhouse, An experiment in systematic study of global seismicity: Centroid-moment tensor solutions for 201 moderate and large earthquakes of 1981, *J. Geophys. Res.*, *88*, 3247–3271, 1983.

Dziewonski, A. M., J. E. Franzen, and J. H. Woodhouse, Centroid-moment tensor solutions for April–June 1983, *Phys. Earth Planet. Inter.*, *33*, 243–249, 1983.

Dziewonski, A. M., J. E. Franzen, and J. H. Woodhouse, Centroid-moment tensor solutions for January–March 1984, *Phys. Earth Planet. Inter.*, *42*, 209–219, 1984.

Dziewonski, A. M., J. E. Franzen, and J. H. Woodhouse, Centroid-moment tensor solutions for January–March 1985, *Phys. Earth Planet. Inter.*, *40*, 249–258, 1985.

Dziewonski, A. M., J. E. Franzen, and J. H. Woodhouse, Centroid-moment tensor solutions for July–September 1985, *Phys. Earth Planet. Inter.*, *42*, 205–214, 1986.

Dziewonski, A. M., G. Ekström, J. E. Franzen, and J. H. Woodhouse, Global seismicity of 1977: Centroid-moment tensor solutions for 471 earthquakes, *Phys. Earth Planet. Inter.*, *45*, 11–36, 1987*a*.

Dziewonski, A. M., G. Ekström, J. E. Franzen, and J. H. Woodhouse, Centroid-moment tensor solutions for January–March 1986, *Phys. Earth Planet. Inter.*, *45*, 1–10, 1987*b*.

Dziewonski, A. M., G. Ekström, J. H. Woodhouse, and G. Zwart, Centroid-moment tensor solutions for October–December 1986, *Phys. Earth Planet. Inter.*, *48*, 5–17, 1987*c*.

Dziewonski, A. M., G. Ekström, J. E. Franzen, and J. H. Woodhouse, Global seismicity of 1982 and 1983: Additional centroid-moment tensor solutions for 553 earthquakes, *Phys. Earth Planet. Inter., 53*, 17–45, 1988*a*

Dziewonski, A. M., G. Ekström, J. E. Franzen, and J. H. Woodhouse, Global seismicity of 1980: Centroid-moment tensor solutions for 515 earthquakes, *Phys. Earth Planet. Inter., 50*, 127–154, 1988*b*

Dziewonski, A. M., G. Ekström, J. H. Woodhouse, and G. Zwart, Centroid-moment tensor solutions for October–December 1987, *Phys. Earth Planet. Inter., 54*, 10–21, 1989*a*

Dziewonski, A. M., G. Ekström, J. H. Woodhouse, and G. Zwart, Centroid-moment tensor solutions for January–March 1988, *Phys. Earth Planet. Inter., 54*, 22–32, 1989*b*

Dziewonski, A. M., G. Ekström, J. H. Woodhouse, and G. Zwart, Centroid-moment tensor solutions for July–September 1988, *Phys. Earth Planet. Inter., 56*, 165–180, 1989*c*.

Dziewonski, A. M., G. Ekström, J. H. Woodhouse, and G. Zwart, Centroid-moment tensor solutions for January–March 1989, *Phys. Earth Planet. Inter., 59*, 233–242, 1990*a*.

Dziewonski, A. M., G. Ekström, J. H. Woodhouse, and G. Zwart, Centroid-moment tensor solutions for April–June 1989, *Phys. Earth Planet. Inter., 60*, 243–253, 1990*b*

Eissler, H. K., and K. C. McNally, Seismicity and tectonics of the Rivera plate and implications for the 1932 Jalisco, Mexico, earthquake, *J. Geophys. Res., 89*, 4520–4530, 1984

Engeln, J. F., D. A. Wiens, and S. Stein, Mechanisms and depths of Atlantic transform earthquakes, *J. Geophys. Res., 91*, 548–577, 1986.

Fisher, R. L., Middle America trench: Topography and structure, *Geol. Soc. Am. Bull., 72*, 703–720, 1961.

Fitch, T. J., Plate convergence, transcurrent faults, and internal deformation adjacent to Southeast Asia and the western Pacific, *J. Geophys. Res., 80*, 4432–4460, 1972.

Fox, P. J., and D. G. Gallo, A tectonic model for ridge-transform-ridge plate boundaries: Implications for the structure of oceanic lithosphere, *Tectonophysics, 104*, 205–242, 1984.

Geist, E. L., J. R. Childs, and D. W. Scholl, The origin of summit basins of the Aleutian Ridge: Implications for block rotation of an arc massif, *Tectonics, 7*, 327–341, 1988.

Goff, J. A., E. A. Bergman, and S. C. Solomon, Earthquake source mechanisms and transform fault tectonics in the Gulf of California, *J. Geophys. Res., 92*, 10,485–10,510, 1987

Harland, W. B., A. V. Cox, P. G. Llewellyn, C. A. G. Pickton, A. G. Smith, and R. Walters, *A Geologic Time Scale*, 131 pp., Cambridge University Press, New York, 1982.

Harrison, C. G. A., and C. A. Johnson, Neotectonics in central Mexico from Landsat TM data, Internal report, 127 pp., Rosenstiel Sch. Mar. and Atmos. Sci., Univ. of Miami, Fla., 1988.

Henderson, L. J., and R. G. Gordon, Mesozoic aseismic ridges on the Farallon plate and southward migration of shallow subduction during the Laramide orogeny, *Tectonics, 3*, 121–132, 1984.

Jarrard, R. D., Terrane motion by strike–slip faulting of forearc slivers, *Geology, 14*, 780–783, 1986.

Johnson, C. A., and C. G. A. Harrison, Tectonics and volcanism in central Mexico: A Landsat Thematic Mapper perspective, *Remote Sens. Envir., 28*, 273-286, 1989.

Kanamori, H. K., Importance of historical seismograms for geophysical research, in *Historical Seismograms and Earthquakes of the World*, edited by W. H. K. Lee, H. Meyers, and K. Shimazaki, pp. 16–33, Academic, San Diego, Calif., 1987.

Klitgord, K. D., Seafloor spreading: The central anomaly magnetization high, *Earth Planet. Sci. Lett., 29*, 201–209, 1976.

Klitgord, K. D., and J. Mammerickx, Northern East Pacific rise: Magnetic anomaly and bathymetric framework, *J. Geophys. Res., 87*, 6725–6750, 1982.

Larson, R. L., Bathymetry, magnetic anomalies, and plate tectonic history of the mouth of the Gulf of California, *Geol. Soc. Am. Bull., 83*, 3345–3360, 1972.

Lonsdale, P., Geology and tectonic history of the Gulf of California, in *The Geology of North America*, Vol. N, *The Eastern Pacific Ocean and Hawaii*, edited by E. L. Winterer, D. M. Hussong, and R. W. Decker, pp. 499–521, The Geological Society of America, Boulder, Colo., 1986.

Lonsdale, P., Structural patterns of the Pacific floor offshore of peninsular California, *Mem. Am. Assoc. Pet. Geol., 47*, in press, 1990.

Luhr, J. F., S. A. Nelson, J. F. Allan, and I. S. E. Carmichael, Active rifting in southwestern Mexico: Manifestations of an incipient eastward spreading-ridge jump, *Geology, 13*, 54–57, 1985.

Macdonald, K. C., K. Kastens, F. N. Spiess, and S. Miller, Deep-tow studies of the Tamayo transform fault, *Mar. Geophys. Res., 4*, 37–70, 1979

Macdonald, K. C., S. P. Miller, S. P. Huestis, and F. N. Spiess, Three-dimensional modeling of a magnetic reversal boundary from inversion of deep-tow measurements, *J. Geophys. Res., 85*, 3670–3680, 1980.

Madsen, J. A., K. C. Macdonald, and P. J. Fox, Morphotectonic fabric of the Orozco fracture zone: Results from a Sea Beam investigation, *J. Geophys. Res., 91*, 3439–3454, 1986

Mammerickx, J., The morphology of propagating spreading ridges, *J. Geophys. Res., 89*, 1817–1828, 1984.

Mammerickx, J., and K. D. Klitgord, East Pacific rise: Evolution from 25 m.y.B.P. to the present, *J. Geophys. Res., 87*, 6751–6758, 1982.

Mammerickx, J., D. F. Naar, and R. L. Tyce, The Mathematician paleoplate, *J. Geophys. Res., 93*, 3025–3040, 1988.

McNally, K. C., and J. B. Minster, Nonuniform seismic slip rates along the Middle America trench, *J. Geophys. Res., 86*, 4949–4959, 1981

Menard, H. W., Fragmentation of the Farallon plate by pivoting subduction, *J. Geol., 86*, 99–110, 1978.

Minster, J. B., and T. H. Jordan, Present-day plate motions, *J. Geophys. Res., 83*, 5331–5353, 1978.

Minster, J. B., and T. H. Jordan, Rotation vectors for the Philippine and Rivera plates (abstract), *Eos Trans. AGU, 60*, 958, 1979.

Minster, J. B., and T. H. Jordan, Vector constraints on Quaternary deformation of the western United States east and west of the San Andreas Fault, in *Tectonics and Sedimentation along the California Margin*, Fieldtrip Guidebook 38, pp. 1–16, edited by J. K. Crouch and S. B. Bachman, SEPM, Pacific Section, Los Angeles, Calif., 1984

Molnar, P., Fault plane solutions of earthquakes and direction of motion in the Gulf of California and on the Rivera fracture zone, *Geol. Soc. Am. Bull., 84*, 1651–1658, 1973.

Molnar, P., and L. R. Sykes, Tectonics of the Caribbean and Middle American region from focal mechanisms and seismicity, *Geol. Soc. Am. Bull., 80*, 1639–1684, 1969.

Moore, D. G., and E. C. Buffington, Transform faulting and growth of the Gulf of California since the late Pliocene, *Science, 161*, 1234–1241, 1968.

Ness, G. E., M. W. Lyle, and R. W. Couch, Marine magnetic anomalies and oceanic crustal isochrons of the gulf and peninsular province of the Californias, *Mem. Am. Ass. Pet. Geol., 47*, in press, 1990.

Nieto-Obregon, J., L. A. Delgado-Argote, and P. E. Damon, Geochronologic, petrologic, and structural data related to large morphologic features between the Sierra Madre Occidental and the Mexican Volcanic Belt, *Geofis. Int., 24*, 623–663, 1985.

Nixon, G. T., The relationship between Quaternary volcanism in central Mexico and the seismicity and structure of subducted ocean lithosphere, *Geol. Soc. Am. Bull., 93*, 514–523, 1982.

Pasquarè, G., V. H. Garduño, A. Tibaldi, and M. Ferrari, Stress pattern evolution in the central sector of the Mexican Volcanic Belt, *Tectonophysics, 146*, 353–364, 1988.

Ross, D. A., and G. G. Shor, Reflection profiles across the Middle America trench, *J. Geophys. Res., 70*, 5551–5572, 1965.

Searle, R. C., Multiple, closely spaced transform faults in fast-slipping fracture zones, *Geology, 11*, 607–610, 1983.

Seno, T., "Northern Honshu microplate" hypothesis and tectonics in the surrounding region, *J. Geod. Soc. Jpn., 31*, 106–123, 1985.

Sharman, G. F., M. S. Reichle, and J. N. Brune, Detailed study of relative plate motion in the Gulf of California, *Geology, 4*, 206–210, 1976.

Singh, S. K., L. Ponce, and S. P. Nishenko, The great Jalisco, Mexico earthquake of 1932 and the Rivera subduction zone, *Bull. Seismol. Soc. Am., 75*, 1301–1314, 1985.

Stein, S., and R. G. Gordon, Statistical tests of additional plate boundaries from plate motion inversions, *Earth Planet. Sci. Lett., 69*, 401–412, 1984

Suarez, G., and S. K. Singh, Tectonic interpretation of the Trans-Mexican Volcanic Belt–Discussion, *Tectonophysics, 127*, 155–160, 1986.

Sykes, L. R., Mechanism of earthquakes and nature of faulting on the mid-ocean ridges, *J. Geophys. Res., 72*, 2131–2154, 1967.

Sykes, L. R., Focal mechanism solutions for earthquakes along the World Rift System, *Geol. Soc. Am. Bull., 60*, 1749–1752, 1970.

Ward, S. N., Pacific–North America plate motions: New results from very long baseline interferometry, *J. Geophys. Res.*, in press, 1990.

C. DeMets, MS 238-332, Jet Propulsion Laboratory, 4800 Oak Grove Drive, Pasadena, CA 91109.

S. Stein, Department of Geological Sciences, Northwestern University, Evanston, IL 60208.

(Received December 7, 1989;
revised August 15, 1990;
accepted August 15, 1990.)